RESEARCH

Open Access

Integrated systems immunology approach identifies impaired effector T cell memory responses as a feature of progression to severe dengue fever

Lisa J. Ioannidis[1,2†], Stephanie I. Studniberg[1,2†], Emily M. Eriksson[1,2], Suhendro Suwarto[3], Dionisius Denis[4], Yang Liao[5], Wei Shi[5], Alexandra L. Garnham[1,6], R. Tedjo Sasmono[4] and Diana S. Hansen[2,7*]

Abstract

Background Typical symptoms of uncomplicated dengue fever (DF) include headache, muscle pains, rash, cough, and vomiting. A proportion of cases progress to severe dengue hemorrhagic fever (DHF), associated with increased vascular permeability, thrombocytopenia, and hemorrhages. Progression to severe dengue is difficult to diagnose at the onset of fever, which complicates patient triage, posing a socio-economic burden on health systems.

Methods To identify parameters associated with protection and susceptibility to DHF, we pursued a systems immunology approach integrating plasma chemokine profiling, high-dimensional mass cytometry and peripheral blood mononuclear cell (PBMC) transcriptomic analysis at the onset of fever in a prospective study conducted in Indonesia.

Results After a secondary infection, progression to uncomplicated dengue featured transcriptional profiles associated with increased cell proliferation and metabolism, and an expansion of ICOS^{+}CD4^{+} and CD8^{+} effector memory T cells. These responses were virtually absent in cases progressing to severe DHF, that instead mounted an innate-like response, characterised by inflammatory transcriptional profiles, high circulating levels of inflammatory chemokines and with high frequencies of CD4^{low} non-classical monocytes predicting increased odds of severe disease.

Conclusions Our results suggests that effector memory T cell activation might play an important role ameliorating severe disease symptoms during a secondary dengue infection, and in the absence of that response, a strong innate inflammatory response is required to control viral replication. Our research also identified discrete cell populations predicting increased odds of severe disease, with potential diagnostic value.

Keywords Dengue fever, Dengue hemorrhagic fever, Effector memory T cells, Non-classical monocytes

†Lisa J. Ioannidis and Stephanie I. Studniberg contributed equally

*Correspondence:
Diana S. Hansen
diana.hansen@monash.edu
Full list of author information is available at the end of the article

Ioannidis *et al. Journal of Biomedical Science*   (2023) 30:24

Page 2 of 21

Background

Dengue is an infection caused by one of four dengue viruses in the family *Flaviviridae*. The virus is transmitted by infected *Aedes aegypti* and *Aedes albopictus*, which are day-biting urban mosquitoes that feed mainly on humans. These vectors are widespread throughout tropical and sub-tropical regions, leaving 70% of the world population at risk of dengue. The disease burden is estimated to 390 million clinical cases per year [1], 500,000 of which are severe enough to require hospitalization. Around 75% of the global population exposed to dengue is in the Asia-Pacific region [2], and the economic cost due to dengue-associated disease in this region has been estimated at US$ 2.36 billion, with a burden of disease as disability-adjusted life years (DALY) of 214,000 ($\sim$ 372 DALYs per million inhabitants) [3, 4].

Dengue virus (DENV) is a positive-sense single-stranded RNA virus, that encodes a polyprotein with three structural proteins and seven nonstructural proteins. The envelope protein (E protein) is involved in receptor binding, membrane fusion, and viral assembly. E protein is the main target of neutralizing antibodies and contains the four DENV serotype-specific antigenic epitopes (DENV-1 to 4). Monocytes, macrophages and dendritic cells in the spleen, lymph nodes, lungs, liver, kidney, and stomach are the primary cellular hosts of DENV in humans [5, 6].

Dengue fever (DF) typically starts from four to seven days after a person is bitten by an infected mosquito. Disease manifests as a sudden onset of fever (up to 40 ºC) that lasts up to ten days and is accompanied by headache and muscle pain in the back and limbs. Other symptoms of moderate dengue include nausea, vomiting, pain in the eyes and rashes on the upper and lower limbs. A proportion of cases can progress to severe dengue also known as dengue hemorrhagic fever (DHF), which is associated with increased vascular permeability leading to thrombocytopenia and hemorrhages. If left untreated this could become life-threatening resulting in severe plasma leakage leading to dengue shock syndrome (DSS), characterized by fluid accumulation causing respiratory distress, severe bleeding and multi-organ failure. There is no specific treatment for dengue, and care is mainly supportive. Oral rehydration and analgesia are routinely used. Intravenous fluids, blood transfusions and intensive care are the required courses of treatment for severe cases. To date, at first presentation, there is no validated way of identifying which individuals will progress to severe manifestations of the disease [7, 8], and in endemic areas, patients are often admitted for inpatient observation, as doctors tend to err on the side of caution. It is estimated that the cost of a non-fatal hospitalized dengue case is US $1394 [3]. Thus, strategies to predict disease progression will not only improve patient management but will also have a substantial socio-economic impact on health systems.

The adaptive immune response plays a key role in protection against DENV, with both T cell-mediated and antibody responses contributing to the control of viral load. Neutralizing antibodies are an important immune defense mechanism against the virus. While primary dengue infection induces a serotype-specific long-lasting neutralizing antibody response able to protect from reinfection [9], cross-reactive antibodies targeted against the other DENV serotypes only protect for a few months [10]. During secondary heterotypic infections, non-neutralizing cross-reactive antibodies from the first infection bind to virions of the second serotype to form DENV-antibody complexes, which are more readily taken up by Fc-gamma-receptor (FcγR)-bearing myeloid cells than uncoated virus particles [11]. This process, known as antibody dependent enhancement (ADE), results in higher levels of viral progeny and has been proposed to lead to severe dengue [12], explaining why secondary DENV infections are usually at higher risk of DHF compared to primary infections.

Similar to antibodies, T cell responses also appear to play a dual role in dengue [13]. CD8$^+$ T cells have been shown to protect against secondary DENV infection in mice and humans [14, 15] and contribute to the antiviral response by killing infected cells and secreting IFN-γ. CD4$^+$ T cells contribute to the control of infection by facilitating B cell and CD8$^+$ T cell activation and secreting cytokines [16]. On the other hand, it has been suggested that CD8$^+$ T cells against a primary DENV serotype can dominate the response to secondary heterotypic infection, resulting in excessive cytokine responses that can worsen disease and induce pathology [17, 18]. It has been also suggested that in heterologous DENV infection, weak affinity cross-reactive CD8$^+$ T cells expand and compete with protective T cells, resulting in inefficient control of the virus and immune pathology [19]. Moreover, DENV-specific CD4$^+$ T cells also produce higher amounts of TNF, a cytokine contributing to disease in DHF patients, in response to heterotypic antigen [20]. To date, the specific phenotypes of T cells associated with protection and susceptibility to severe dengue have not been fully defined.

The fact that antibody-mediated and T cell-mediated responses appear to participate in both protection from infection and dengue pathogenesis has complicated the identification of reliable correlates of immunity, which poses a caveat in the evaluation of effective anti-DENV vaccines. These considerations have also deterred the identification of cellular parameters or biomarkers to predict the clinical course of disease. To address these

Ioannidis *et al. Journal of Biomedical Science*   (2023) 30:24

Page 3 of 21

issues, we pursued a systems biology approach integrating plasma chemokine profiling, high-dimensional mass cytometry and peripheral blood mononuclear cell (PBMC) transcriptional profiling in a prospective study of individuals from a dengue-endemic area that progressed to develop either DF or DHF. High frequencies of CD4^{low} non-classical monocytes were associated with progression to DHF and predicted increased odds of severe disease at the onset of fever. Progression to severe dengue was also associated with a transcriptional signature featuring impaired T cell activation and reduced cell metabolism compared to individuals with mild disease manifestation. In contrast, uncomplicated dengue cases featured an expansion of ICOS^{high}CD4$^+$ and CD8$^+$ effector memory T cells. Our research suggests that efficient T cell activation might play a critical role in attenuating severe disease symptoms during secondary DENV infections. The results also provide proof of concept for the potential of systems biology approaches to identify immunological signatures predicting increased odds of DHF to develop diagnostic tools for early detection of complicated cases.

Methods
Study population
A prospective, observational study of dengue cases was conducted at Pondok Indah Hospital in Jakarta, Indonesia. A dengue positive diagnosis was confirmed by detection of DENV NS1 antigen at point of care (SD Bioline, Korea). RT-PCR to determine DENV serotype was done using the Simplexa Dengue Real-time RT-PCR Kit (DiaSorin, Salugglia, Italy). The four DENV serotypes were found among participants, with DENV-2 being the most prevalent (58%), followed by DENV-4 (18%) and DENV-1/-3 (12% each). Consenting participants with a confirmed diagnosis (aged between 16 and 64 years) donated a venous blood sample at first presentation (day 1–3 of fever), and plasma and PBMCs were frozen. Virus-specific IgM and IgG antibodies were measured in plasma samples collected at first presentation using Panbio Dengue Duo IgM and IgG Capture ELISA (Alere), to classify cases between primary and secondary infections based on the IgM/IgG ratio. Participants with a positive IgM and negative IgG result were classified as primary infections, while secondary infections were identified by a positive IgG which could be accompanied by positive IgM result. Participants were monitored daily for disease progression (DF or DHF) for 10 days as previously described [21]. Based on routine laboratory tests and clinical evaluation, the attending physicians classified the dengue disease grade based on 2011 WHO guidelines [22]. Briefly, cases with clinical symptoms, including headache, retro-orbital or abdominal pain, vomiting,

fluid accumulation, evidence of skin or mucosal bleed, liver enlargement and an increase in haematocrit with a concurrent rapid reduction of platelet count (below 10×10^3/ml) were classified as DHF.

Luminex assay for chemokine assessment
Chemokines from uninfected healthy controls and confirmed dengue cases were quantified in plasma samples by Luminex® (R&D systems) assay. Magnetic beads were formulated into pre-designed microparticle cocktails with capture antibodies against human CCL2, CCL17, CXCL5, CXCL8, CXCL9, CXCL10 and CXCL11. Dilutions for reagents, standards, and samples were performed following the manufacturer's protocol. Diluted samples, standards, and microparticle cocktails were added to microplate wells and incubated for 2 h at 22 °C with agitation. After washing three times with washing buffer, a biotin-antibody cocktail was added, and plates were incubated for an additional hour at 22 °C. After three washes, samples were incubated in the presence of a streptavidin-PE conjugate for 30 min. After a final wash, plates were read using a Luminex 100/200 instrument with xPONENT software (Luminex Corp., Austin, TX, USA). Mean fluorescence intensity values were used to estimate chemokine concentration, extrapolating from standard curves.

Cytometry by time-of-flight
PBMCs ($1–2 \times 10^6$) from DF and DHF cases as well as non-infected dengue-naive Melbourne controls were stained with 5 µM Cell-ID Cisplatin (Fluidigm) in PBS for 5 min at room temperature. Cells were then blocked with Human TruStain FcX (Biolegend) and stained with a cocktail of surface marker antibodies (Additional file 1: Table S1) in CyTOF staining buffer (PBS with 0.5% bovine serum albumin [BSA; Sigma] and 0.02% sodium azide [Sigma]) for 30 min at room temperature. After surface staining, cells were washed twice with CyTOF staining buffer and then incubated with 125 nM Cell-ID iridium intercalator (Fluidigm) in Maxpar fix and perm buffer (Fluidigm) for a minimum of 18 h. Prior to data acquisition, cells were washed twice by centrifugation in ultrapure water and then resuspended in a 1/10 dilution of 4-Element EQ normalization beads (Fluidigm) in ultrapure water. Cells were analysed on a Helios model mass cytometer (Fluidigm) at ∼300 events/s. Data were normalized using the signal from 4-Element EQ Beads (Fluidigm) as previously described [23]. Manual gating was then performed using FlowJo version 10 (BD Biosciences) to exclude doublets and dead cells, before individual cell populations were selected and exported for further analysis in Cytobank [24]. Individual cell populations were then visualized using viSNE [25], while

Ioannidis *et al. Journal of Biomedical Science*   (2023) 30:24

Page 4 of 21

FlowSOM [26] was used to identify cell sub-populations. Self-organizing maps (SOMs) were generated for each cell population using hierarchical consensus clustering on the tSNE axes. The parameters included in each viSNE analysis are shown in Additional file 2: Table S2. CITRUS [27] was used to identify differentially abundant cell populations using the same parameters as the viSNE analysis at a 1% false-discovery rate (FDR).

RNA-sequencing

RNA was extracted from 2×10^5 PBMCs from selected samples with sufficient material to allow assessment of multiple endpoints using the RNeasy Plus Mini Kit (QIAGEN) following manufacturers' instructions. RNA was quantified with RNA Screen Tape on the Agilent TapeStation 2200 System. Libraries were prepared with either 50 ng or 25 ng of total RNA using the Illumina TruSeq RNA Library Prep Kit (< 100 ng) v1.0 following manufacturers' instructions and submitted for sequencing by paired end, 80 bp reads on an Illumina NextSeq 500 platform.

Transcriptional analysis

Raw sequence reads in FASTQ file format were aligned to the human reference genome GRCh38/hg38 using the align() function in Rsubread version 2.10.5 with default parameters [28, 29]. Fragments of aligned sequences overlapping Gencode human genes (GRCh38.p13) were quantified with featureCounts [30], with Gencode version 38 primary assembly annotation used in the quantification. Genes with no symbols, sex-linked genes, immunoglobulin genes, and non-protein-coding genes were filtered out from the analysis. Haemoglobin genes were found to be highly variable and were also filtered from the analysis. Genes with low counts in fewer than 5 samples were determined as unexpressed and filtered out using the filterByExpr function in edgeR version 3.38.4 [31], leaving 13,013 genes for differential expression analysis. Filtered counts were normalised using the trimmed mean of M-values method [32] in edgeR. A design matrix was constructed incorporating the group, and adjusting for day from fever onset as follows:

$$\text{design} \leftarrow \text{model.matrix}(0 + \text{group} + \text{feverday}).$$

Counts were transformed to log2-CPM (logCPM), precision weighted and quantile normalised using the voomwithQualityWeights() function to down-weight within-group variability [33, 34] in limma version 3.52.2 [35]. A linear model was fitted to each gene and differential expression was assessed using robust empirical Bayes moderated *t*-statistics [36] with a cut-off of 5% applied

for calling differentially expressed genes. Entrez Gene IDs for differentially expressed genes were entered into the goana() and kegga() functions [37] in limma to determine over-representation of differentially expressed genes in Gene Ontology (GO) terms. Lists of differentially expressed genes between pairwise comparisons were also entered into the Ingenuity Pathway Analysis software platform (QIAGEN Inc., https://www.qiagenbioinformatics.com/products/ingenuity-pathway-analysis) for canonical pathway and upstream regulator analysis. Differential enrichment of functional immune pathways was determined using the tmodLimmaTest() function in the tmod package version 0.46.2 [38] with blood transcription modules [39] and hallmark gene signatures from the molecular signatures database (mSigDB) [40, 41] as gene sets. Significant GO pathways were visualised using the GOPlot package version 1.0.2 [42]. Heatmaps were generated using the pheatmap (version 1.0.12) and ComplexHeatmap (version 2.12.1) [43] packages, and chord diagrams were generated using the circlize package version 0.4.15 [44] Rotational gene set testing and barcode plots were generated using the limma package in R [35].

Statistical analysis

Characteristics of clinical groups were compared using unpaired t-tests or ANOVA for continuous data that was normally distributed, while Mann–Whitney tests or Kruskal Wallis tests were used for data that did not follow normal distribution. Chi-squared tests were used to evaluate nominal data. The false discovery rate was controlled to below 5% using the method of Benjamini and Hochberg [45] throughout the study. Correlations were determined using Spearman's rank correlation as indicated and visualised using the network_plot() function in the corrr package version 0.4.4. Logistic regression models were fitted between groups to determine the odds ratio for cell populations. Hierarchical clustering heatmaps were calculated using the complete method and Euclidian distance matrix. Statistical analyses were performed in GraphPad prism version 9 and R version 4.2.0.

Results

Cohort characteristics

The clinical characteristics of the study participants are summarised in Fig. 1. The study recruited individuals with a confirmed dengue positive diagnosis. Study participants with a confirmed secondary DENV infection were selected for this analysis. Consenting participants donated a venous blood sample at enrolment (day 1–3 of fever) and were then monitored daily for disease progression to DF or DHF for 10 days as described in Methods. There was no difference in age or gender composition between study participants (Fig. 1A, B) and viral loads
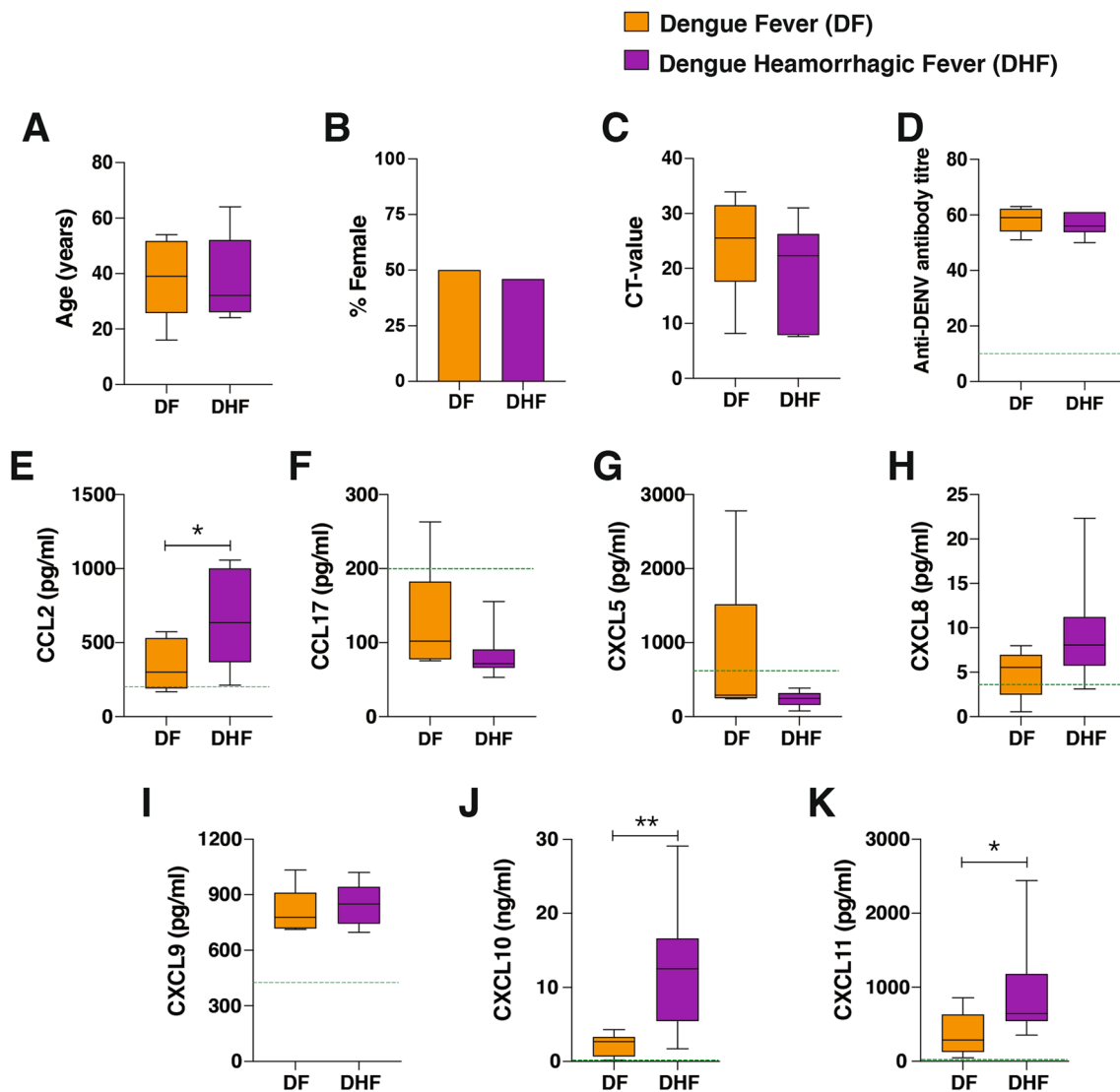
Fig. 1 Study cohort characteristics. Individuals with a confirmed secondary DENV infection were recruited for the study at the onset of fever and followed up for progression to DF (n = 7) or DHF (n = 10). **A–D**. Clinical parameters determined in the study include age (**A**), gender (**B**) and CT-value (**C**), and anti-DENV IgG antibody titres (**D**). Boxes represent the 25th to 75th percentiles, whiskers show the range (minimum to maximum), and lines represent the median of biological replicates. The dotted line depicts the average antibody background levels of uninfected healthy controls (n = 5). Line plots depict mean ± SD. Significance was determined by the Kruskal–Wallis test (**A**), the Chi-square test (**B**), and the Mann-Whitney test (**C**, **D**), *p < 0.05. **E–K**. Mean chemokine levels. CCL2 (**E**), CCL17 (**F**), CXCL5 (**G**), CXCL8 (**H**), CXCL9 (**I**), CXCL10 (**J**) and CXCL11 (**K**) were determined in plasma samples of study participants. Boxes represent the 25th to 75th percentiles, whiskers show the range (minimum to maximum), and lines represent the median of 7 (DF) and 10 (DHF) biological replicates. The dotted line depicts the average antibody background levels of uninfected healthy controls (n = 5). Significance was determined by the Mann-Whitney test. *p < 0.05, **p < 0.01

were similar between clinical groups (Fig. 1C). Assessment of antibody responses to the DENV envelope protein at first presentation revealed that all DF and DHF cases had high virus-specific IgG titres (Fig. 1D). Plasma chemokine levels were also assessed at first presentation. CCL17, CXCL5 and CXCL8 levels in both clinical groups were similar to background levels in healthy controls. While CXCL9 levels were comparable in DF and DHF cases, CCL2, CXCL10 and CXCL11 levels were increased in DHF cases compared with the DF group (Fig. 1E–K). Thus, all individuals in this arm of the study have a confirmed secondary DENV infection, and individuals progressing to severe illness produced high levels of inflammatory chemokines at the onset of fever.

Ioannidis *et al. Journal of Biomedical Science*   (2023) 30:24

Page 6 of 21

High-dimensional mass cytometry identifies lymphocyte sub-populations associated with different dengue disease outcomes

To identify lymphocyte sub-populations associated with progression to DF or DHF after a secondary DENV infection, PBMCs of study participants collected at the onset of fever were stained with a panel of metal-labelled antibodies against a range of B cell, T cell, Natural Killer (NK) cell and monocyte markers (Additional file 1: Table S1) and analysed by cytometry by time of flight (CyTOF). Within the circulating memory $CD4^+$ T cell compartment, surface expression of the chemokine receptors CCR6 and CXCR3 allows the identification of T helper $(T_H)_1$-like $(CCR6^-CXCR3^+)$, T_{H2}-like $(CCR6^-CXCR3^-)$ and T_{H17}-like $(CCR6^+CXCR3^-)$ cells, while circulating memory T follicular helper (T_{FH}) cells can be identified by expression of CXCR5 (Additional file 3: Fig. S1). To explore the composition of these memory $CD4^+$ T cell populations, tSNE analysis and FlowSOM clustering were performed, and marker expression was assessed in each cell population. This approach allowed for the identification of five distinct sub-populations of T_{H1} memory $CD4^+$ T cells, T_{H2} memory $CD4^+$ T cells, T_{H17} memory $CD4^+$ T cells and memory T_{FH} cells expressing variable levels of chemokine receptors and surface markers including CCR7, ICOS, PD-1, CD25, CD27 and CD127 (Fig. 2A–D). A similar approach was used to explore the composition of the memory $CD8^+$ T cell pool, with six distinct sub-populations identified (Fig. 2E).

Within the circulating memory B cell (MBC) pool, CD21 and CD27 expression can be used to identify classical MBCs $(CD27^+CD21^+)$ and atypical MBCs $(CD27^-CD21^-)$. tSNE analysis and FlowSOM clustering of the $CD19^+CD20^+CD10^-$ MBC pool facilitated the identification of five classical and three atypical MBC sub-populations, including populations of both IgM^+IgD^+ and class-switched (IgM^-IgD^-) cells expressing variable levels of the chemokine receptors CCR6, CCR7, CXCR3 and CXCR5 (Fig. 2F), present in the blood of dengue patients at first presentation. Within the innate cell compartment, FlowSOM clustering of gated $CD14^+$ monocytes revealed two classical $(CD14^+CD16^-)$, two intermediate $(CD14^+CD16^{low})$ and one non-classical $(CD14^+CD16^{high})$ monocyte sub-population (Fig. 2G) in the blood of dengue patients. Four sub-populations expressing different levels of CD16 were also identified among $CD3^-CD56^+$ NK cells (Fig. 2H).

The frequency of each cell sub-population identified by FlowSOM clustering was determined. Unsupervised hierarchical clustering (Fig. 2I) and multi-dimensional scaling (Fig. 2J) of all sub-populations segregated most DF and DHF cases. Four main groups of cell populations

were identified by unsupervised hierarchical clustering, with trends towards cell populations more abundant in cases progressing to DHF in clusters 1 and 2, and cell populations preferentially expressed among individuals progressing to DF in clusters 3 and 4 (Fig. 2I). Interestingly, cluster 4 included classical monocytes as well as sub-populations of memory T_{FH} cells, T_{H1} and T_{H2}-polarised $CD4^+$ T cells expressing high levels of inducible T cell costimulatory (ICOS), programmed cell death protein 1 (PD-1) and CD27. Spearman correlation analysis indicated that frequencies of these T cell populations (marked in brown in Fig. 2K) were highly correlated with each other (Fig. 2K). In contrast, subsets of memory T_{FH} cells, T_{H1}, T_{H2} and T_{H17} polarised $CD4^+$ T cells in clusters 1–2 (marked in purple in Fig. 2K), apparently enriched among individuals progressing to DHF, were also correlated with each other and were characterized by high expression levels of CCR7 and CD127.

To further explore these responses, unsupervised identification of differentially abundant cell populations between clinical groups was performed using the CITRUS algorithm [27] (FDR < 1%). This analysis identified two populations of memory T_{H1}-polarised $CD4^+$ T cells differentially abundant between clinical groups. $ICOS^+PD-1^+CD27^+CCR7^-$ cells were virtually absent in DHF cases. These cells, resembling an effector memory phenotype, were highly abundant in individuals that progressed to DF. In contrast, $CD127^+$ cells were significantly higher in DHF cases relative to DF counterparts (Fig. 3A). A highly similar pattern was observed in the memory T_{H2} $CD4^+$ T cell pool, with a subset of $ICOS^+PD-1^+CD27^+CCR7^-$ cells significantly higher in DF compared to DHF cases and $CD127^+$ cells enriched in DHF individuals compared to those with mild disease (Fig. 3B). Furthermore, the same population of $ICOS^+PD-1^+CD27^+CCR7^-$ cells was also identified as significantly higher in DF compared to DHF cases in the memory T_{H17}-$CD4^+$ T cell compartment (Fig. 3C). CITRUS analysis also identified one population of $CXCR3^+$ memory T_{FH} cells and an additional population of $CXCR3^+$ memory $CD8^+$ T cells significantly more abundant in DF compared to DHF cases, also displaying high levels of ICOS, PD-1, and CD27 (Fig. 3D, E). Thus, together these results suggest that during a secondary infection, progression to uncomplicated dengue is associated with the expansion of $CD4^+$ and $CD8^+$ T cells consistent with an effector memory phenotype and expressing high levels of co-stimulatory molecules.

CITRUS analysis revealed two populations of MBCs differentially abundant between clinical groups. Whereas $CXCR5^+CCR6^+$ class-switched classical MBCs were higher in DF individuals, class-switched atypical MBCs
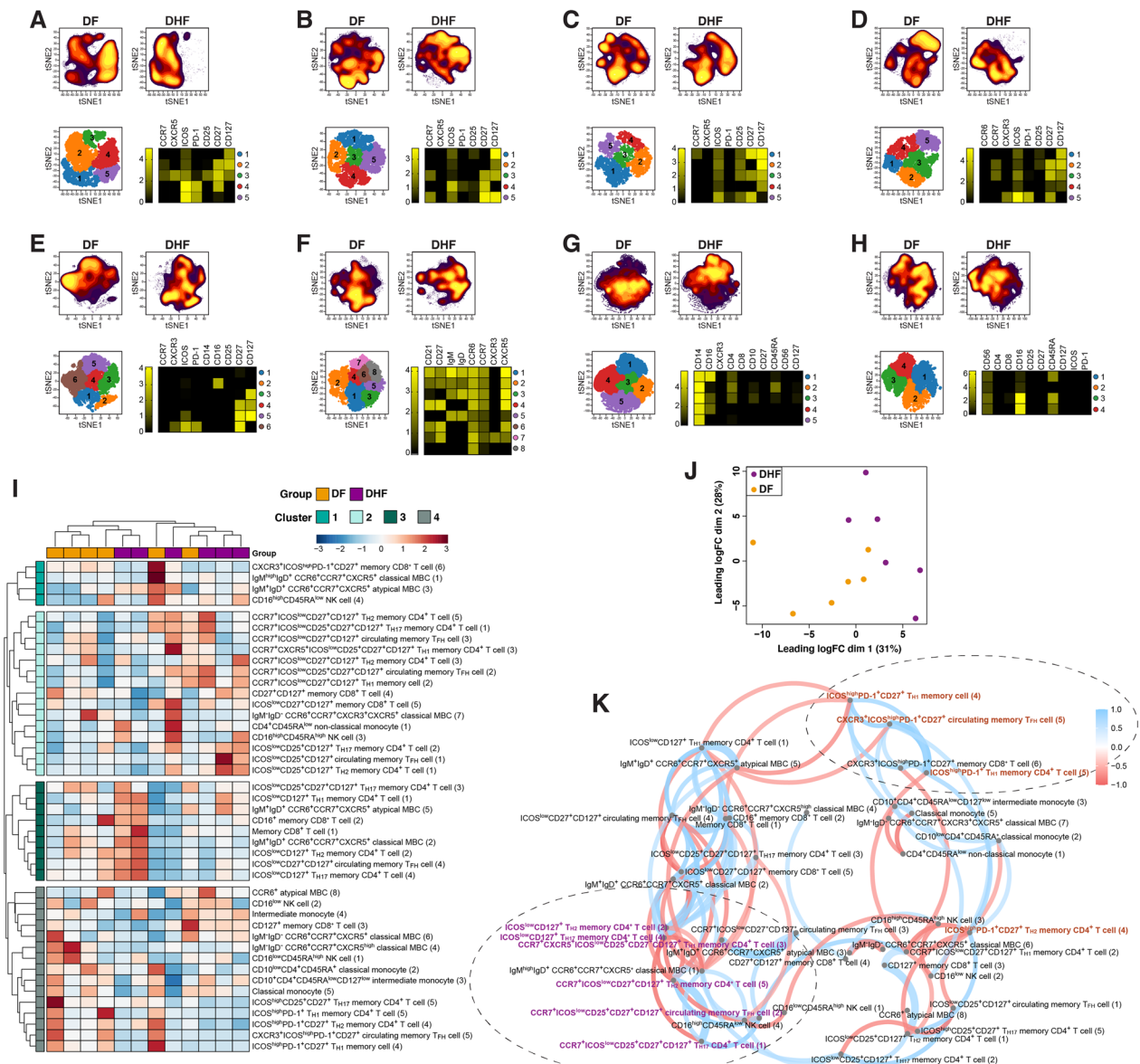
Ioannidis *et al. Journal of Biomedical Science*   (2023) 30:24

Page 7 of 21

Fig. 2 Identification of memory CD4$^+$ and CD8$^+$ T cells, MBCs, monocyte and NK cell sub-populations in DENV-infected individuals. **A–K** PBMCs collected at first presentation from DENV-positive individuals progressing to DF (n=6) or DHF (n=6) were stained with a panel of metal-labelled antibodies and analysed by CyTOF. tSNE analysis was performed and FlowSOM clustering was used to identify individual cell sub-populations within gated: **A** T$_{H1}$ memory CD4$^+$ T cells (CD19$^-$CD3$^+$CD4$^+$CD45RA$^-$CCR6$^-$CXCR3$^+$), **B** T$_{H2}$ memory CD4$^+$ T cells (CD19$^-$CD3$^+$CD4$^+$CD45RA$^-$CCR6$^-$CXCR3$^-$), **C** T$_{H17}$ memory CD4$^+$ T cells (CD19$^-$CD3$^+$CD4$^+$CD45RA$^-$CCR6$^+$CXCR3$^-$), **D** Circulating memory T$_{FH}$ cells (CD19$^-$CD3$^+$CD4$^+$CD45RA$^-$CXCR5$^+$), **E** Memory CD8$^+$ T cells (CD19$^-$CD3$^+$CD8$^+$CD45RA$^-$). **F** MBCs (CD3$^-$CD19$^+$CD20$^+$CD10$^-$), **G** Monocytes (CD3$^-$CD19$^-$CD14$^+$), **H**. NK cells (CD3$^-$CD19$^-$CD14$^-$CD56$^+$). The tSNE plots in the top panel display cell density and represent the pooled data for each group, while the lower panel shows a projection of the FlowSOM clusters on a tSNE plot. Heatmaps show the median marker expression for each FlowSOM cluster. **I** Unsupervised hierarchical clustering heatmap showing the frequency of all FlowSOM clusters across all clinical samples. **J** Unsupervised multi-dimensional scaling of all populations identified by FlowSOM clustering across all clinical samples. **K** Spearman correlation networks were used to examine the relationship between cell populations identified by FlowSOM clustering induced in response to infection. Blue lines represent positive correlations, and red lines represent negative correlations. The distance between variables is determined by multidimensional scaling and represents the strength of the correlation, where highly correlated variables are positioned closer together
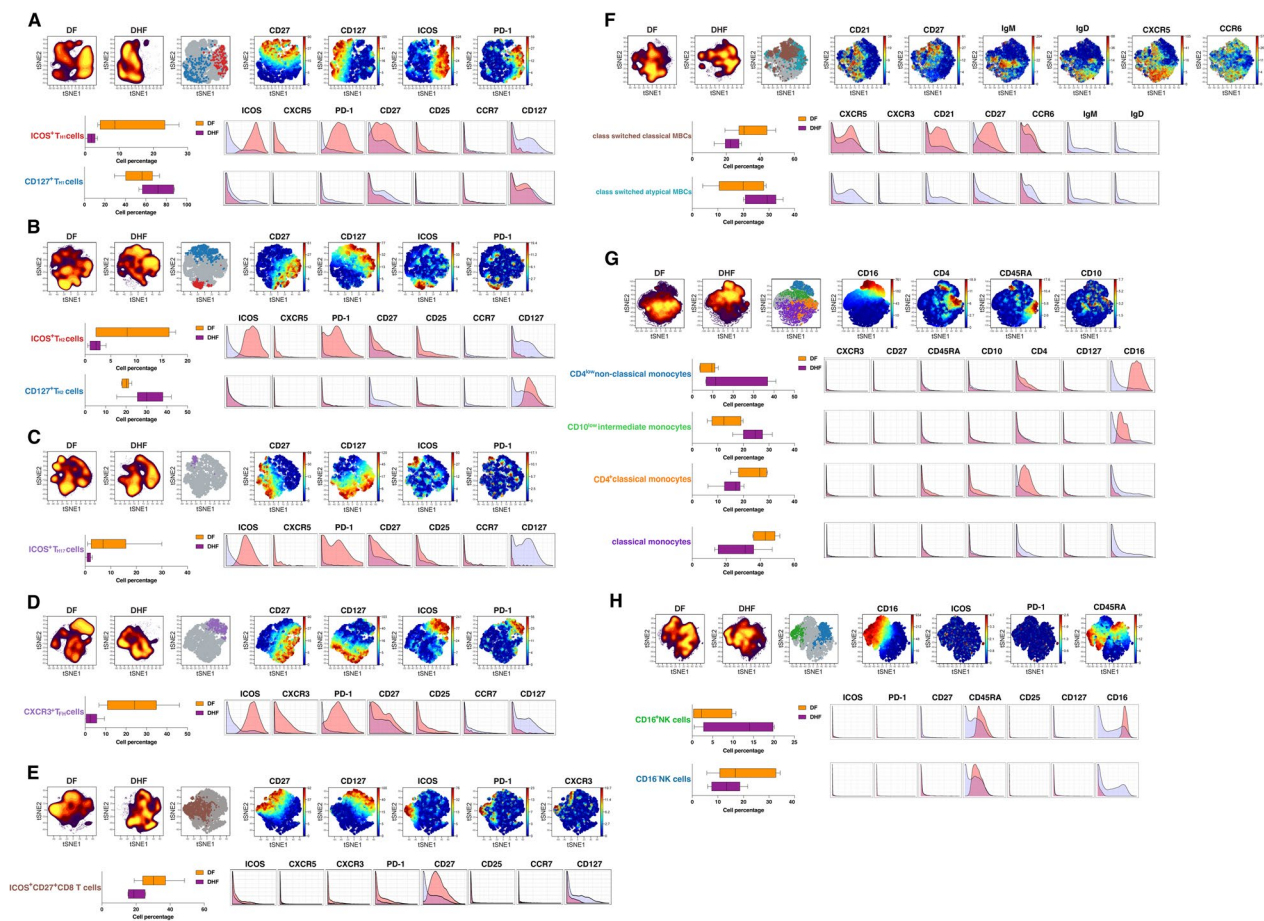
Fig. 3 Subsets of T cells, MBCs, monocytes and NK cells associated with progression to different dengue fever outcomes. **A–H**. Unsupervised identification of differentially abundant cell populations between DF (n = 6) or DHF (n = 6) clinical groups was performed using CITRUS (FDR < 1%). Differentially abundant populations were identified among: (**A**) T_H1 memory CD4+ T cells; (**B**) T_H2 memory CD4+ T cells; (**C**) T_H17 memory CD4+ T cells; (**D**) circulating memory T_FH cells; (**E**) memory CD8+ T cells; (**F**) MBCs; (**G**) monocytes; (**H**) NK cells. The tSNE plots in the top of each panel display cell density and represent pooled data for each clinical group as calculated in the clustering analysis shown in Fig. 2A-G, while the middle panels show differentially abundant populations identified in colours on a tSNE overlay, and the viSNE plots on the left-hand side from each top panel depict relevant marker expression on tSNE overlays. The lower left panels show the frequency of differentially abundant cell populations identified by CITRUS. Boxes represent the 25th to 75th percentiles, whiskers show the range (minimum to maximum), and lines represent the median of 6 (DF) and 6 (DHF) biological replicates. The lower right panels illustrate marker expression in differentially abundant populations (pink histograms), relative to background expression (lilac histograms)

were significantly enriched in DHF cases compared to DF counterparts (Fig. 3F). In the monocyte compartment, classical monocytes and CD4+ classical monocytes were significantly higher in DF compared to DHF cases, while a population of CD4^low non-classical monocytes and a population of CD10^low intermediate monocytes were higher in individuals that developed DHF (Fig. 3G). Moreover, highly abundant in patients progressing to DHF was a subset of CD16+ NK cells, whereas their CD16− counterparts were significantly higher in DF cases (Fig. 3H). Importantly, downstream analysis of the 15 populations identified as differentially abundant by CITRUS using manual gating, showed that except for classical MBCs, CD4+ classical monocytes (which were significantly reduced in DHF cases), and CD16+ NK cells, blood frequencies of all cell types were negligible among dengue-naive healthy controls compared to dengue-exposed study participants (Additional file 3: Fig. S2), confirming the expansion of these cellular compartments in response to DENV infections progressing to different disease outcomes. Thus, whereas CD16+ NK cells and non-classical monocytes appear to be associated with progression to severe dengue, T_H1-polarised T_FH cells and ICOS^high CD4+ and CD8+ effector memory T cells are features associated with more favourable infection outcomes after a secondary DENV infection.

Ioannidis *et al. Journal of Biomedical Science*   (2023) 30:24

Page 9 of 21

RNA sequencing of PBMCs at the onset of fever segregates transcriptional profiles of individuals progressing to DF or DHF

To identify molecular pathways associated with progression to DF or DHF, selected study participants with sufficient material were chosen for transcriptional profiling by RNA-sequencing (RNA-seq). Multi-dimensional scaling and unsupervised hierarchical clustering of transcriptional profiles discriminated between individuals progressing to DF and DHF (Fig. 4A, B). A design matrix was created with clinical groups as a factor with adjustment for day of fever upon hospital presentation. The design matrix was then incorporated into linear modelling and gene expression estimation for the identification of differentially expressed genes between DHF and DF. A total of 2411 genes were found to be differentially expressed, with 929 upregulated and 1482 downregulated in patients progressing to DHF compared with patients progressing to DF (Fig. 4B). To identify immunological processes underlying differences in transcriptional profiles, differential enrichment was assessed with the gene set enrichment tool tmod [38], using pairwise comparisons between clinical groups and blood transcriptional modules (BTMs) [39] as gene sets (Fig. 4C, D). Modules involved in type-I interferons, apoptosis and an NK cell signature were significantly enriched in DHF compared to DF cases. Conversely, modules involved in cell division, cell cycle, glycolysis, oxidative phosphorylation as well as plasma cells were significantly underrepresented in cases progressing to severe DHF compared to DF counterparts.

Progression to DHF features transcriptional profiles supporting innate inflammatory responses, reduced cell division and reduced oxidative metabolism relative to DF

To further define transcriptional signatures preferentially activated by individuals progressing to DF or DHF, various platforms were pursued for gene set enrichment analysis (Fig. 5A–D). Gene ontology (GO) terms (Fig. 5B), Kyoto Encyclopedia of Genes and Genomes (KEGG) pathways (Fig. 5C), and Ingenuity Pathway Analysis (IPA) (Fig. 5D) showed significant upregulation of pathways involved in innate immune response to microorganisms in individuals progressing to DHF. This included genes encoding several cytokine/chemokines and cytokine/chemokine receptors such as *IL1R1*, *IL7R*, *CCL8* and *CXCL11*, signalling molecules and

transcription factors governing the stress response such as *JAK2* and *GATA2*, various guanylate-binding proteins (*GBP1, GBP4, GBP5*), all IFN-γ-inducible proteins known to exert anti-microbial activity, along with *TLR3*, a toll like receptor responsible for recognition of double stranded RNA. Furthermore, genes encoding protein products involved in apoptosis, such as *FAS, FASLG* and *CD274* (also known as programmed death-ligand 1), and metalloproteinases (*MMP8, MMP9*), upregulated in various pathogenic conditions, were also among the genes upregulated in patients progressing to DHF.

Upstream regulator analysis identified increased activation of rapamycin-insensitive companion of mTOR (*RICTOR*) and La-related protein 1 (*LARP1*) pathways in DHF compared to DF patients (Fig. 5E). Both pathways are critical in the control of mTOR signalling that governs cell proliferation and metabolism and have been shown to be modulated by viral infections to support viral replication [46–48]. The transcription regulator Non-POU domain-containing octamer-binding protein [49] as well as the cytokine IFN-alpha-2 (*IFNA2*) and its receptor *IFNAR* were also upstream regulators in patients progressing to DHF, with several genes involved in stress response and inflammatory processes predicted as targets in these type I IFN-mediated pathways (Fig. 5E). A graphical summary, used to identify the main entities featured by transcriptional profiles of DHF cases predicts that *TLR3* activation (recognising viral RNA) activates this inflammatory cytokine response, resulting mainly in NK cell and monocyte activation, a strong antimicrobial response and downstream inhibition of viral replication (Fig. 5F).

Two main signature pathways appeared to be downregulated in individuals progressing to DHF and enriched in patients with milder disease manifestations: cell proliferation and cell metabolic processes including, oxidative phosphorylation, cellular respiration and glycolysis. These included genes encoding cyclins such as *CCNB1* and *CCNB2*, cell activation marker *MKI67*, replication factors such as *PCNA* and *CDC20*, as well as transcriptional regulator *FOXM1* (Fig. 5A–D). Genes encoding several enzymes critical for cell metabolic processes such as *GAPDH, NDUFB7, NDUFS5* as well as *ATP5MC3*, *ATP51F1* and *ATP5PF* required for ATP metabolism, were also reduced in DHF compared to DF patients. Upstream regulator and graphical summary analysis predicted key transcription factors involved in the control of

(See figure on next page.)

Fig. 4 RNA-seq of PBMCs segregates transcriptional profiles of individuals progressing to DF or DHF. **A–D** PBMCs collected at first presentation from DENV-positive individuals progressing to DF (n=5) or DHF (n=6) were selected for RNA-seq analysis. **A** Unsupervised multi-dimensional scaling of the top 500 most variably expressed genes across all samples. **B** Unsupervised hierarchical clustering of the 2411 differentially expressed genes between DF and DHF cases using the complete method and Euclidian measure of distance. **C–D** tmod gene set enrichment analysis showing significant BTMs differentially enriched for pairwise comparisons (FDR < 5%).
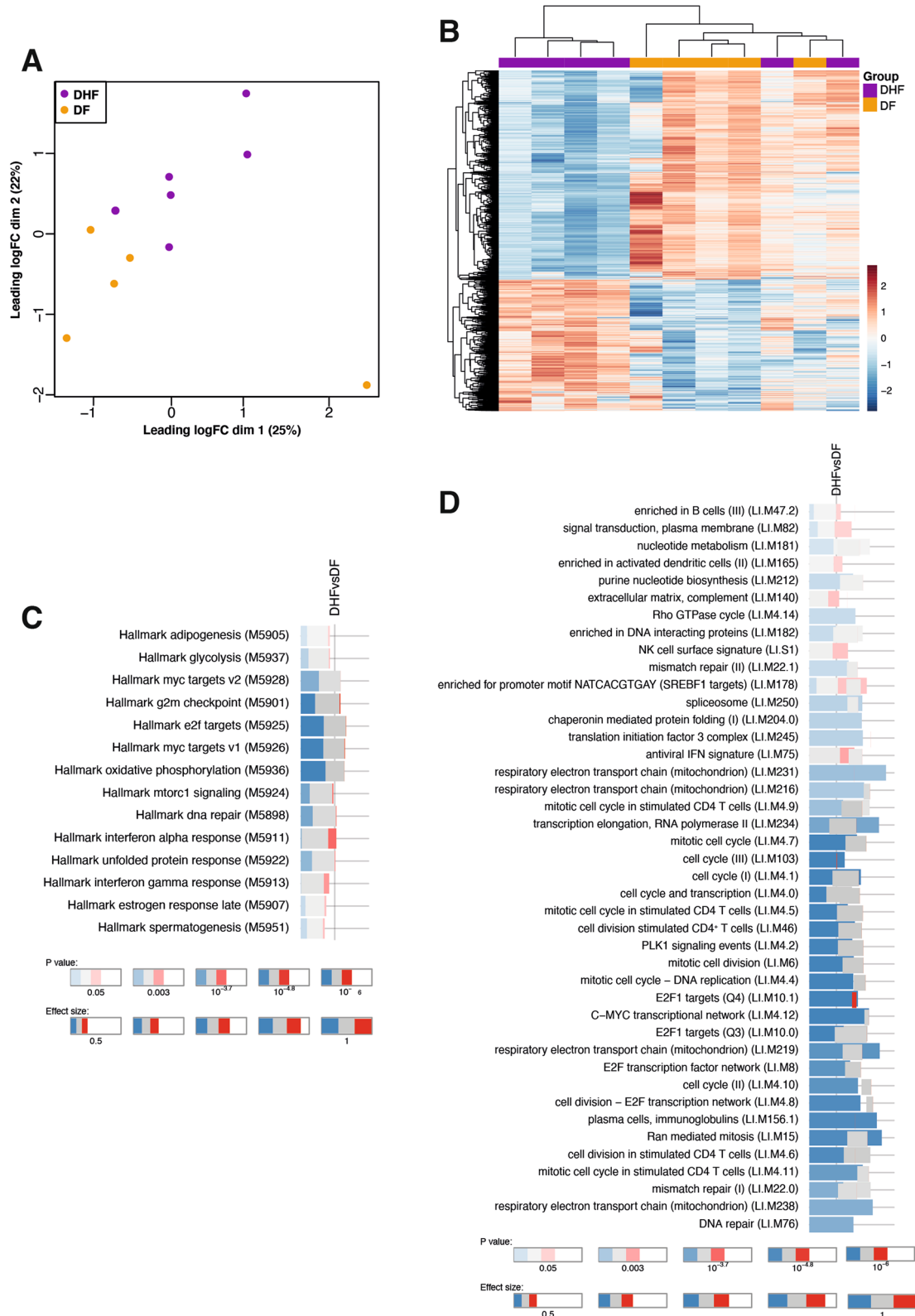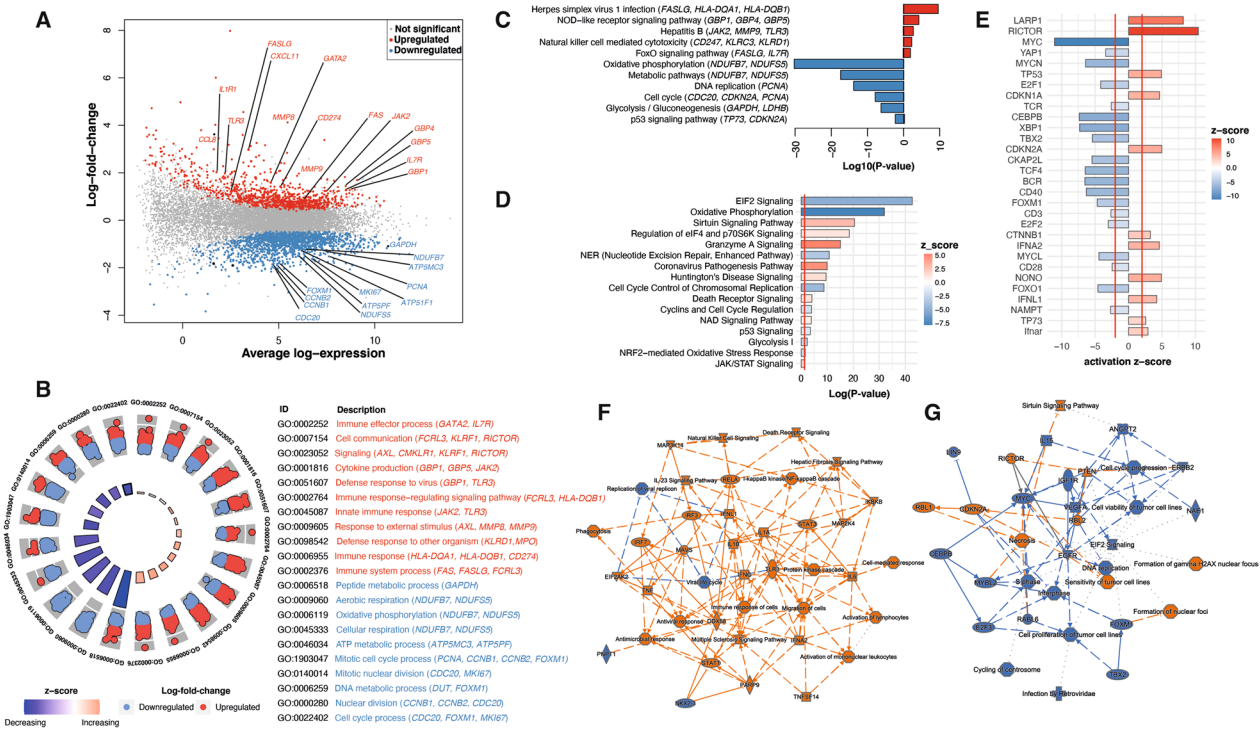
Fig. 4 (See legend on previous page.)

Fig. 5 Transcriptional profiles supporting inflammatory processes and reduced cell proliferation and metabolism in individuals progressing to DHF. **A–G** Gene expression profiles of PBMCs from DENV-infected individuals progressing to DF (n = 5) or DHF (n = 6) were compared. **A** Mean-difference plot displaying genes differentially expressed between DF and DHF cases. Each gene is plotted as a single point determined by log-fold-change and average transcript abundance. Red genes are overrepresented, and blue genes are underrepresented in DHF relative to DF. **B** Plots showing significantly enriched GO terms scaled by Log10(P-value). Red GO terms are upregulated and blue GO terms are downregulated in DHF compared to DF. **C** Bar plots showing significantly enriched KEGG pathways scaled by Log10(P-value). Red KEGG pathways are upregulated and blue KEGG pathways are downregulated in DHF compared to DF. **D** IPA canonical pathways significantly overrepresented in differentially expressed genes between DF and DHF cases scaled by Log10(P-value). Pathways with a positive z-score in red are activated in DHF relative to DF, and pathways with a negative z-score in blue are inhibited in DHF compared to DF. The red line corresponds to a P value of 0.05. **E** Upstream regulator analysis of the 2411 differentially expressed genes between DHF and DF. The red lines represent a significant activation z-score of ±2. **F–G** Graphical summaries depicting networks of genes and downstream processes activated in cases progressing to DHF relative to DF (**F**) or processes enriched in patients progressing to DF relative to DHF (**G**)

cell division such as *MYC, FOXM1* and *FOXO1*, as well as T cell activation molecules (*CD3, CD40*, and *CD28*) as key elements responsible for these transcriptional signatures, suggesting that these pathways could become preferentially activated in individuals who progressed to mild DF (Fig. 5D, G).

To address this, and to specifically confirm that these pathways modulated before the onset of DF or DHF are enriched or diminished relative to homeostatic transcriptional levels of healthy uninfected controls, we compared our list of 2411 differentially expressed genes with a previously described transcriptional signature of 1303 genes differentially expressed upon unclassified DENV infection relative to uninfected controls [50]. This analysis identified a significant enrichment of 393 genes in common between both data sets (Additional file 3: Fig. S3A–C). Notably, gene set enrichment of these 393 genes using GO terms, KEGG pathways,

and IPA showed identical transcriptional signatures compared to the results in Fig. 5, with an innate-like anti-viral stress response featuring upregulation of TNF and type-1 interferons before progression to DHF, and a significant enrichment of terms involved in cell proliferation, cell metabolism, and T cell activation in individuals that did not develop severe hemorrhagic symptoms. Thus, together these results suggest that after a secondary DENV infection, progression to DHF is associated with an innate immune transcriptional signature as well as impaired activation and expansion of the T cell compartment.

Since other studies have previously analysed transcriptional profiles of cases progressing to DF or DHF in other locations, we sought to determine if our results were aligned with findings obtained in different settings. To that end, we identified two multi-cohort analyses [51, 52] that together integrated 12 unique gene expression

Ioannidis *et al. Journal of Biomedical Science*   (2023) 30:24

Page 12 of 21

datasets [53–64] capturing 466 [51] and 365 [52] clinical samples of patients progressing to DF or DHF (Additional file 3: Fig. S4A). Whereas the first multi-cohort analysis framework discovered a 20-gene set predictive of severe dengue, the second one identified an 8-gene predictive signature. Importantly, the accuracy of these signatures was validated in independent prospective cohort studies. When these two gene signatures were combined and compared with our list of 2411 differentially expressed genes, rotational gene set testing using the ROAST test in limma [35] revealed a significant enrichment (p < 0.01) of 10 genes from the 28-gene signature (Additional file 3: Fig. S4B, C, D). Gene set enrichment analysis of these shared genes using GO terms showed transcriptional profiles featuring innate and antimicrobial humoral immunity (Additional file 3: Fig. S4E). Thus, despite the limitations of a small sample size, our findings appear to be significantly aligned with validated gene signatures predicting progression to DHF.

Uncomplicated dengue fever transcriptional profiles correlate with effector memory T cell responses to DENV infection
To integrate immune responses associated with progression to DF or DHF identified by CyTOF and blood transcriptional signatures, Spearman correlations (Benjamini-Hochberg adjusted FDR < 5%) were applied (Fig. 6A, B). For this analysis, genes identified to be under the control of signature upstream regulators identified in Fig. 5 by IPA analysis were used. In general, cell populations overrepresented in individuals progressing to DF were positively correlated with the proliferation/metabolism and T cell activation transcriptional signatures, with ICOS$^+$ memory T_{H1} and T_{H17} cells, as well as CXCR3$^+$ T_{FH} cells featuring the highest number of associations with gene expression profiles (Fig. 6A). Hierarchical clustering of these transcriptional signatures confirmed that most of the differentially expressed genes in the data set predicted to be under the control of upstream regulators *MYC* and *FOXM1* were upregulated in cases progressing to DF

compared to DHF and featured GO terms specifically associated with cellular metabolic processes (Fig. 6C, D). Nearly half of the genes predicted to be under the control of upstream regulators *CD3, CD28* and *CD40* were upregulated in DF relative to DHF cases (Fig. 6E). Gene set enrichment analysis revealed that whereas terms involved in lymphocyte activation were upregulated in DF cases, genes encoding protein products supporting apoptosis and IFN-γ responses were upregulated in cases progressing to DHF (Fig. 6F).

In general, the inflammatory transcriptional signature featured by cases progressing to DHF was negatively correlated with cell clusters abundant in DF cases, but showed positive associations with cell populations overrepresented in DHF cases, with CD4^{low} non-classical monocytes and memory CD127$^+$ T_{H1} cells showing the highest number of correlations (Fig. 6B). The 10-gene set shared between our differentially expressed gene list and multi-cohort defined gene signatures [51, 52] also showed positive correlations with atypical MBCs, abundant among DHF cases (Additional file 3: Fig. S5). Almost all these genes, under the control of upstream regulators *NONO, IFNA2* and *IFNAR* and featuring GO terms involved in antiviral and inflammatory cytokine response, were clearly upregulated in individuals progressing to DHF compared to DF counterparts. Thus, together these findings suggest that the expansion of the effector memory CD4$^+$ and CD8$^+$ T cell pool observed in DF cases (Figs. 2, 3) might be supported by increased metabolic rates, required to induce activation and proliferation of this compartment, and in the absence of this adaptive response, a type-I innate response is required to control the infection, which is associated with progression to severe disease manifestations.

The balance between classical and non-classical circulating monocytes predicts risk of DHF after primary and secondary DENV infection
Figures 2, 3, 4, 5 and 6 suggest that in the absence of robust effector memory T cell responses in DHF cases, a

(See figure on next page.)
Fig. 6 Integrative analysis of cellular signatures and transcriptional profiles in cases progressing to DF or DHF. **A** Chord diagram integrating associations between DF signature genes, immune cell populations and chemokine responses. Blue lines within the chord diagram represent positive correlations between two variables, while red lines represent negative correlations. (Benjamini-Hochberg adjusted Spearman's Rho, FDR < 5%). **B** Chord diagram integrating associations between DHF signature genes, immune cell populations and chemokine responses. Blue lines within the chord diagram represent positive correlations between two variables, while red lines represent negative correlations. (Benjamini-Hochberg adjusted Spearman's Rho, FDR < 5%). **C** Hierarchical clustering heatmap of genes predicted to be under the control of upstream regulators *MYC* and *FOXM1* amongst patients progressing to DF or DHF. **D** Bar plots showing significantly enriched GO terms scaled by Log10(P-value) for genes in heatmap in C. **E** Hierarchical clustering heatmap of genes predicted to be under the control of upstream regulators *CD3, CD28* and *CD40* amongst patients progressing to DF or DHF. **F** Bar plots showing significantly enriched GO terms scaled by Log10(P-value) for genes in heatmap in E. Red GO terms are upregulated and blue GO terms are downregulated in DHF compared with DF. **G** Hierarchical clustering heatmap of genes predicted to be under the control of upstream regulators *NONO, IFNA2* and *IFNAR* amongst patients progressing to DF or DHF. **H** Bar plots showing significantly enriched GO terms scaled by Log10(P-value) for genes in heatmap in G
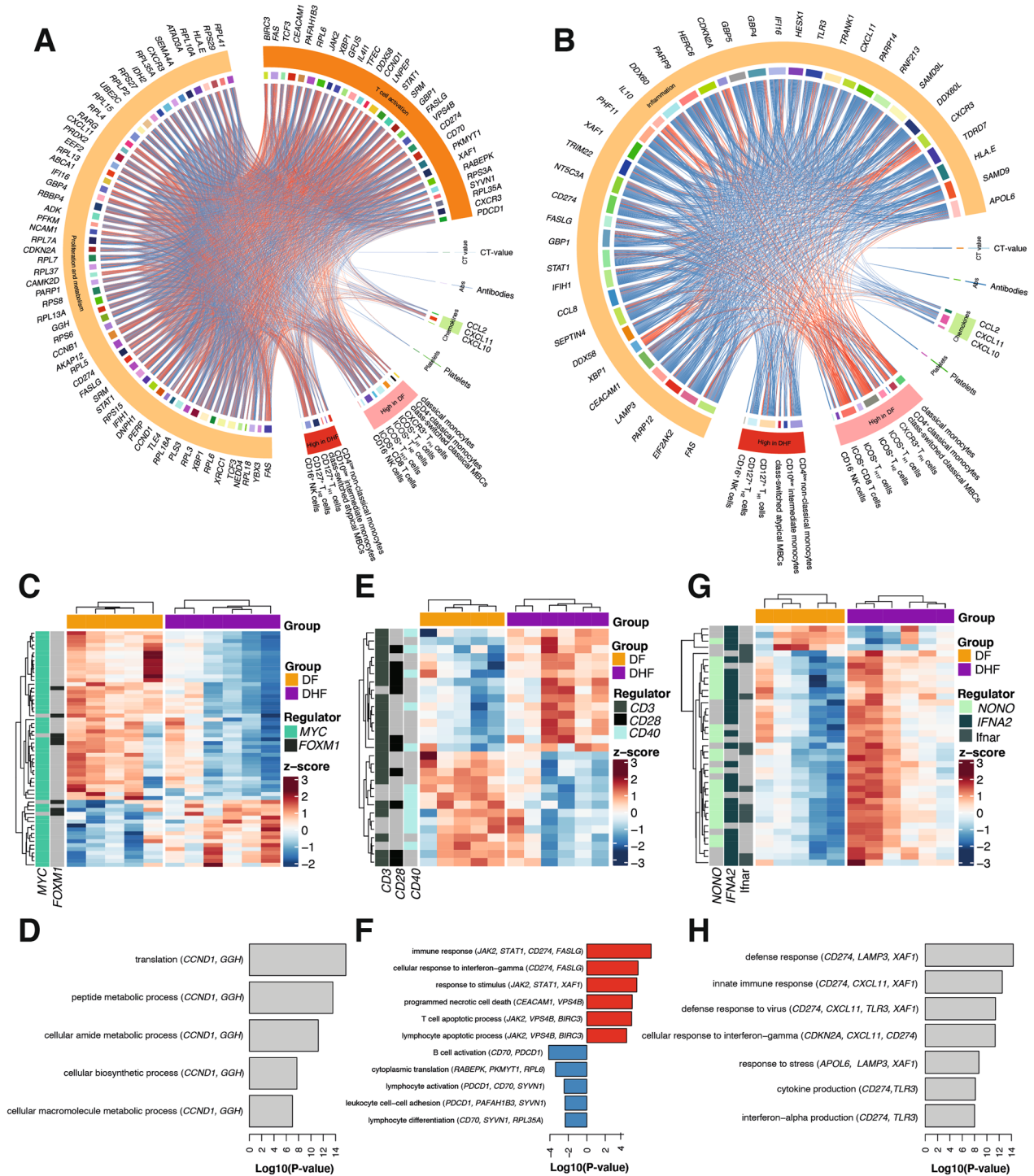
Fig. 6 (See legend on previous page.)

innate immune response, including activation of NK cells and monocytes is the main defence against the virus during a secondary DENV infection. Therefore, we sought to determine (1) whether a similar response pattern was observed in cases progressing to DHF after a primary

DENV infection, and (2) if defined innate cell populations in the blood could be good predictors of odds of severe hemorrhagic illness at the onset of fever. To that end, PBMCs collected at first presentation from participants that had a confirmed primary DENV infection

(high IgM and no detectable IgG virus-specific antibodies) were stained with a panel of metal-labelled antibodies against monocyte and NK cell markers (Additional file 1: Table S1) and analysed by CyTOF.

The clinical characteristics of the primary infection arm of the study were similar to those with secondary infection and are summarized in Additional file 3: Fig. S6. There was no difference in age or gender composition between study participants (Additional file 3: Fig. S6B), with a trend towards higher viral loads that did not reach significance in DHF cases (Additional file 3: Fig. S6C). Unlike the secondary infection arm of the cohort that identified high levels of some chemokines in cases progressing to DHF, no significant differences were found in plasma CCL17, CXCL5, CXCL8 and CXCL9, CCL2, CXCL10 and CXCL9 levels between clinical groups (Additional file 3: Fig. S6D–J).

To explore the composition of innate cells after primary DENV infection, tSNE analysis and FlowSOM clustering were performed within gated monocytes (Fig. 7A) as well as $CD3^-CD56^+$ NK cells (Fig. 7B), and marker expression was assessed in each cell population. Similar to our findings after secondary infection, this analysis revealed two classical ($CD14^+CD16^-$), two intermediate ($CD14^+CD16^{low}$) and one non-classical ($CD14^+CD16^{high}$) monocyte sub-population (Fig. 7A) in the blood of primary dengue cases. Four subsets of NK cells, expressing different levels of CD16 were also identified by FlowSOM clustering (Fig. 7B). The CITRUS algorithm was then applied for unsupervised identification of differentially abundant cell populations between clinical groups (FDR < 1%). Whereas no differentially abundant populations of NK cells were found, similar to secondary infection, $CD4^+$ classical monocytes were significantly higher in individuals developing DF compared to cases progressing to DHF, and $CD4^{low}$ non-classical monocytes were highly abundant in cases that progressed to DHF (Fig. 7C).

Next, all samples from the primary and secondary arms of the study were combined, and tSNE and FlowSOM analysis performed to obtain frequencies of all monocyte and NK cell sub-populations across the entire cohort (Additional file 3: Fig. S7). To define associations between cell populations and risk of developing DHF, logistic regression models were applied (Benjamini-Hochberg adjusted FDR < 5%). Whereas high frequencies of $CD4^+$ classical and $CD4^+CD10^+CD45RA^+$ intermediate monocytes were associated with reduced odds of DHF, high frequencies of $CD4^{low}$ non-classical monocytes predicted increased odds of progressing to DHF at the onset of fever (Fig. 7D). The frequencies of these cell populations were then assessed for their ability to classify individuals progressing to DF or DHF. Figure 7E F show the ROC curve and predicted frequencies of the best performing model. Circulating levels of $CD4^+$ classical and $CD4^{low}$ non-classical monocytes were able to correctly classify individuals developing either DF or DHF with a high degree of accuracy (AUROC 0.8455, p = 0.0075), providing proof of concept for the potential of defined monocyte populations in the blood identified by single cell approaches to predict odds of severe dengue at the onset of fever.

Discussion

Secondary DENV infections are usually more severe than a primary exposure to the virus and are a well-accepted risk factor for DHF and DSS [65]. A large body of data supports the concept that exposure to DENV results in the development of protective as well as disease-enhancing adaptive immune responses upon re-infection, with both antibody-mediated and T cell responses contributing to these processes [9, 11, 16–18, 66]. To untangle the complexity of this immunological landscape, this study pursued a systems biology approach integrating clinical parameters, plasma chemokine levels, high-dimensional mass cytometry, and blood transcriptional profiling in

(See figure on next page.)

Fig. 7 High frequencies of circulating $CD4^{low}$ non-classical monocytes predict increased odds of DHF. **A–C** PBMCs collected at first presentation from DENV-positive individuals progressing to DF (n = 5) or DHF (n = 4) after a primary infection were stained with a panel of metal-labelled antibodies and analysed by CyTOF. tSNE analysis was performed and FlowSOM clustering was used to identify individual cell sub-populations within gated $CD3^-CD19^-CD14^+$ monocytes (**A**) and $CD3^-CD19^-CD14^-CD56^+$ NK cells (**B**). The tSNE plots in top panels display cell density and represent the pooled data for each group, while the lower panel shows a projection of the FlowSOM clusters on a tSNE plot. Heatmaps show the median marker expression for each FlowSOM cluster (**C**). Differentially abundant populations were identified by CITRUS among gated monocytes. The top panels show differentially abundant populations identified in colours on a tSNE overlay, and the viSNE plots on the right-hand side from each top panel depict relevant marker expression on tSNE overlays. The lower left panels show the frequency of differentially abundant cell populations identified by CITRUS. Boxes represent the 25th to 75th percentiles, whiskers show the range (minimum to maximum), and lines represent the median of 6 (DF) and 6 (DHF) biological replicates. The lower right panels illustrate marker expression in differentially abundant populations (pink histograms), relative to background expression (lilac histograms). **D** Odds ratios as determined by logistic regression showing associations between cell frequencies and the risk of progressing to DHF. Symbols represent the odds ratio estimated using 10 patients progressing to DHF, and 11 patients progressing to DF after primary or secondary infection. The vertical lines depict the 95% confidence interval. *p < 0.05, **p < 0.01. **E–F** ROC curve (**E**) and predicted probability plot (**F**) classifying individuals progressing to DF (n = 11) or DHF (n = 10) at first presentation based on the frequency of $CD4^+$ classical monocytes and $CD4^{low}$ non-classical monocytes
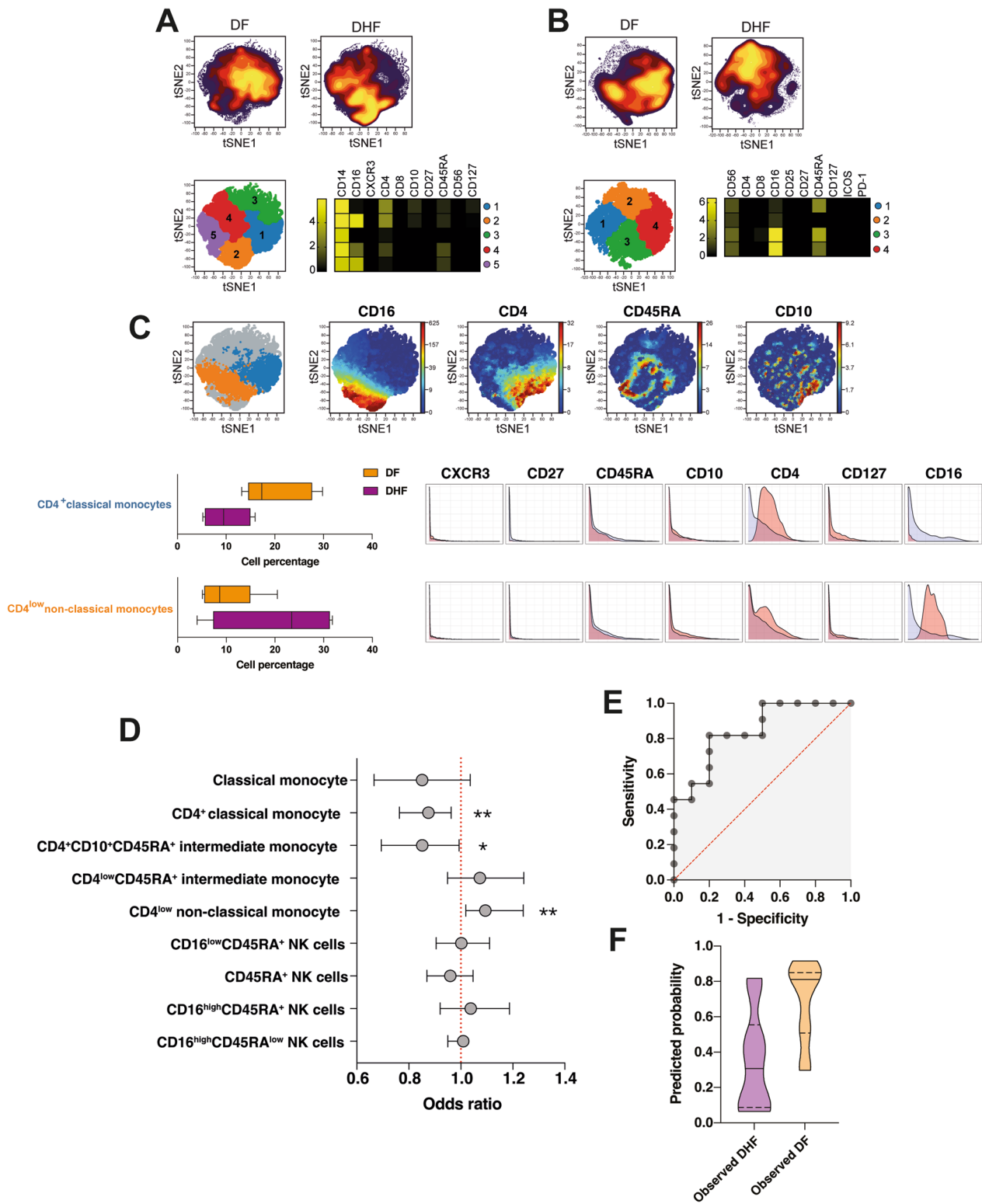
Ioannidis *et al. Journal of Biomedical Science* (2023) 30:24

Page 15 of 21

Fig. 7 (See legend on previous page.)

Ioannidis *et al. Journal of Biomedical Science*　　(2023) 30:24

Page 16 of 21

adults from a dengue-endemic area in Indonesia to identify cellular and molecular processes associated with progression to DF or DHF after a second exposure to DENV. We found that whereas progression to uncomplicated disease manifestations was associated with increased cell proliferation and metabolism transcriptional profiles and an expansion of $CD4^+$ and $CD8^+$ effector memory T cells, progression to severe DHF featured a type-I immune response characterised by inflammatory transcriptional profiles as well as high circulating levels of inflammatory chemokines and non-classical monocytes. Thus, our results are consistent with a model in which effector memory T cell activation could play an important role to ameliorate severe disease during a secondary DENV infection, and in the absence of these processes, a strong innate response is required to control viral replication, at the expense of producing an inflammatory environment that contributes to the induction of clinical symptoms.

Over the past decade, numerous studies investigated transcriptional profiles of dengue cases to identify markers of disease progression, with varied results. Similar to our findings here, progression to severe dengue has been shown to be often [52, 53, 57, 59, 67–69] but not always [54, 58, 61, 70] associated with transcriptional signatures featuring NK cell activation, increased apoptosis, upregulation of type I interferon and IFN-γ-mediated pathways. In contrast to this innate-like inflammatory transcriptional response associated with progression to DHF, our bioinformatic analysis identified T cell activation molecules and master transcription factors such as *MYC*, *FOXM1* and *FOXO1*, known to support cell proliferation and govern a range of metabolic processes, as regulators of transcriptional profiles in patients progressing to uncomplicated disease manifestations. These gene expression profiles were tightly correlated with frequencies of $ICOS^+$ effector memory T cells and $CXCR3^+$ T_{FH} cells, lending support to the idea that the increased metabolic transcriptional signature observed had developed to support the energy demands of a proliferating T cell pool, which was expanding upon a secondary encounter with the virus.

Elegant longitudinal studies demonstrated that both effector memory $CD4^+$ and $CD8^+$ T cells are induced after exposure to DENV and that these cells are long-lived, persisting for 12 months post-infection [71–73]. Consistent with those findings, our high-dimensional single-cell cytometry analysis identified various populations of $ICOS^+PD-1^+CD27^+CCR7^-$ T_{H1}, T_{H2} and T_{H17}-polarised $CD4^+$ T cells as well as $CD8^+$ T cells with an effector memory phenotype only 2–3 days after the onset of fever, suggesting the prior presence and rapid expansion of these cells upon a secondary DENV

infection. Notably, these cells were only present in individuals progressing to mild disease manifestations and virtually absent in patients that developed DHF. Similarly, transcriptional profiles of asymptomatic DENV-infected individuals [62] featured increased T cell activation relative to clinical dengue counterparts, and multi-functional $CD4^+$ and $CD8^+$ T cells have been found at higher frequencies in outpatients compared to hospitalized dengue cases [74]. Together, this evidence supports the concept that adaptive T cell immunity, and particularly effector memory T cells, might play a critical role in attenuating disease severity during a secondary DENV infection and associate with good infection outcomes. In our study, all effector memory $CD4^+$ and $CD8^+$ T cell subsets found in individuals progressing to uncomplicated dengue expressed high level of co-stimulatory molecules, including ICOS. Expression of this co-stimulatory molecule is usually found in various T cell types, including T regulatory cells, T_{FH} cells and effector T cells. In these cells, ICOS plays an important role in cell activation, maintenance, and survival [75]. Emerging research is highlighting the importance of ICOS co-stimulation to deliver efficient anti-tumour effector T cell responses [76–78], with various ICOS agonist antibodies currently in clinical trial showing promising results [79, 80]. Targeting this co-stimulatory pathway could be also beneficial to boost adaptive immunity and improve disease outcomes in secondary dengue infections.

Unsupervised analysis of the B cell compartment identified a subpopulation of $CD21^-CD27^-$ atypical MBCs preferentially expanded in DHF cases. These cells have been detected in other viral [81] and parasitic [82] infections and share features in common with a subset called age-associated B cells [83]. In these settings, atypical MBCs have been found to have low differentiating capacity into antibody-secreting cells upon re-encounter with antigen and similar to our results here, associations with poor disease outcomes [83, 84, 85]. In contrast, class-switched classical MBCs dominated the response in individuals progressing to DF. Although anti-DENV antibody titres in the study were comparable across individuals with different infection outcomes, our results do not exclude the possibility that antibodies with different neutralising capacity and/or affinity for antigen could arise after stimulation and differentiation of these MBC subsets present in DF or DHF cases and play a role in the progression towards different clinical outcomes.

$CXCR5^+CD4^+$ circulating memory T_{FH} cells have been shown to provide help to B cells and share many functional features with T_{FH} cells in the lymphoid organs [86]. These cells have been previously found to become

activated in response to DENV and to correlate with plasmablast frequencies [87, 88]. Similar to conventional T helper cells, the expression of the lineage-defining chemokine receptors CXCR3 and CCR6 allows the differentiation of T_{H1}-, T_{H2}- and T_{H17}-polarised memory T_{FH} cells, and previous findings suggested that CXCR3 expression in T_{FH} cells is associated with their functional capacity. Although it was initially proposed that CXCR3$^+$ cells have reduced helper capacity compared to CXCR3$^-$ cells [89], CXCR3$^+$ T_{FH} cells have been also found to succesfully expand and secrete cytokines, particularly in response to various viral infections [90, 91]. Consistent with these findings, our analysis here identified a population of CXCR3$^+$ T_{FH} cells correlating with classical MBCs and only present in study participants with mild disease manifestations. Further work will be required to determine if CXCR3$^+$ T_{FH} cells provide help to support the production of efficient neutralising antibody responses that protect against severe dengue disease symptoms.

Monocytes are one of the main targets of DENV and several studies have assessed the relative abundance of classical, intermediate and non-classical subsets during acute infection [56, 92–94]. How the composition of this compartment fluctuates in patients with different disease severity in DENV infections is less understood. Here, using unsupervised high-dimensional data analysis, we found that whereas populations of classical monocytes are abundant at the onset of fever in individuals developing uncomplicated dengue, non-classical monocytes dominate the blood response in patients progressing to DHF, suggesting that these cells could contribute to the induction of severe clinical symptoms. In support to this idea, non-classical monocytes have been shown to upregulate expression of adhesion molecules and chemokine receptors that facilitate endothelial cell adhesion [94] in response to acute DENV infection. These cells are also major producers of pro-inflammatory cytokines including TNF, IL-1β, and IL-6 [95]. TNF is a potent activator of the vascular endothelium known to modulate the permeability of endothelial cells [96], raising the possibility that local production of TNF by non-classical monocytes could contribute to vascular leakage in DHF cases. Non-classical monocytes may also promote ADE by supporting the differentiation of B cells into plasmablasts [56] that produce short-lived, low affinity antibodies and have been identified as one of the main cellular targets of DENV in the blood that becomes activated in severe cases [68].

The currently used warning signs to identify dengue cases at risk of developing severe ilness are based on clinical parameters that appear late in the disease and are not always specific. This situation promotes ineffective patient triage and resource allocation [7, 8]. Recent studies estimated that the total cost per hospitalized dengue case raises to US$1,250 [97] in Indonesia, with the total economic burden associated to hospitalized dengue cases estimated to US$355.2 million [97]. Thus, strategies to predict the burden of disease will have a substantial socio-economic impact in dengue endemic regions. From all parameters induced in response to DENV identified by our systems biology approach, the balance between defined populations of classical and non-classical monocytes in the blood was the best predictor of odds of DHF after 1–3 days of fever. Furthermore, unlike inflammatory chemokines, CD4^{low} non-classical monocytes were detectable in cases progressing to DHF, not only after secondary but also primary DENV infections, in which other risk factors such as cross-reactive antibodies cannot be detected.

Conclusions
Despite the limitations of a small sample size, this prospective study provided new insights on processes associated with favourable disease outcomes and protection from severe dengue upon a second encounter with DENV. Thus, single cell cytometry approaches combined with molecular profiling like the one presented here could be useful to help identify correlates of protection and define disease-protecting CD4$^+$ and CD8$^+$ T cell phenotypes that emerging anti-DENV vaccines under efficacy testing could aim to reproduce. The results also provide proof of concept for the potential of systems immunology approaches to identify discrete populations in the blood associated with increased odds of DHF, encouraging more granular examination of these cell compartments to identify specific biomarkers, useful for the design of diagnostic tools to predict disease outcomes of patients presenting with dengue fever at point of care.

Abbreviations

DF	Dengue fever
DHF	Dengue hemorrhagic fever
PBMC	Peripheral blood mononuclear cell
DALY	Disability-adjusted life years
DENV	Dengue virus
FcγR	Fc-gamma-receptor
ADE	Antibody dependent enhancement
ICOS	Inducible T cell co-stimulator
PD-1	Programmed cell death protein 1
CyTOF	Cytometry by time of flight
tSNE	t-distributed stochastic neighbour embedding
SOMs	Self-organizing maps
CITRUS	Cluster identification, characterization, and regression
Th cell	T helper cell
Tfh cell	T follicular helper cell
MBC	Memory B cell
NK cell	Natural killer cell
RNA-seq	RNA-sequencing
BTMs	Blood transcriptional modules
IPA	Ingenuity pathway analysis
GO	Gene ontology

Ioannidis *et al. Journal of Biomedical Science*   (2023) 30:24

Page 18 of 21

KEGG	Kyoto Encyclopedia of Genes and Genomes
GBP	Guanylate-binding protein
TLR3	Toll like receptor 3
MMP	Metalloproteinase
RICTOR	Rapamycin-insensitive companion of mTOR
LARP1	La-related protein 1
NONO	Non-POU domain-containing octamer-binding protein
IFNAR	Interferon-alpha receptor

Supplementary Information

The online version contains supplementary material available at https://doi.org/10.1186/s12929-023-00916-4.

Additional file 1: **TableS1:** CyTOF antibodies. Antibodies used for deep immunophenotyping in the study.

Additional file 2: **TableS2:** Cell surface makers included as parameters in viSNE analysis. Surface markers used for unsupervised high-dimensional analysis of major blood cell populations.

Additional file 3: **Fig.S1.** Gating strategy to define major memory T cell, MBC, monocyte and NK cell populations. **Fig. S2.** Relative percentage of populations differentially abundant between DF and DHF cases identified by CITRUS in dengue-naive healthy controls. **Fig. S3.** Comparison of transcriptional profiles of DF and DHF cases relative to transcription levels of uninfected healthy controls. **Fig. S4.** Comparison of transcriptional profiles of DF and DHF cases with two gene signatures predictive of progression to severe dengue. **Fig. S5.** Correlation analysis of a 10-gene set predictive of severe dengue with clinical parameters, chemokine levels and cellular signatures found in dengue cases. **Fig. S6.** Primary dengue study cohort characteristics. **Fig.S7.** Monocyte and NK cell sub-populations induced in DENV-infected individuals progressing to DF or DHF.

Availability of data and materials
Processed bulk RNA-seq data generated for this study are available as GEO series (GSE215835). Raw data are available upon request, subject to approval by our Institutional Data Access Committee (dataaccess@wehi.edu.au) to ensure preservation of patient confidentiality.

Declarations

Ethics approval and consent to participate
The study was approved by the Human Research Ethics Committees of the Eijkman Institute for Molecular Biology, Jakarta, Indonesia, the Health Research Ethics Committee - Faculty of Medicine Universitas Indonesia and Cipto Mangunkusumo Hospital (HREC-FMUI/CMH), The Walter and Eliza Hall Institute of Medical Research, and Monash University in Australia. Written informed consent was obtained from all study participants prior to their inclusion in the study. All the experiments conformed to the principles set out in the WMA Declaration of Helsinki and the Department of Health and Human Services Belmont Report.

Consent for publication
Not applicable.

Competing interests
The authors declare no competing interests.

Author details
[1]The Walter and Eliza Hall Institute of Medical Research, Parkville, VIC, Australia. [2]Department of Medical Biology, The University of Melbourne, Parkville, VIC, Australia. [3]Division of Tropical and Infectious Diseases, Department of Internal Medicine, Faculty of Medicine, Universitas Indonesia, Cipto Mangunkusumo National Hospital (RSCM), Jakarta, Indonesia. [4]Eijkman Research Center for Molecular Biology, Jakarta, Indonesia. [5]Olivia Newton-John Cancer Research Institute, Heidelberg, VIC, Australia. [6]School of Mathematics and Statistics, The University of Melbourne, Parkville, VIC, Australia. [7]Department of Microbiology, Monash Biomedicine Discovery Institute, Monash University, Clayton, VIC, Australia.

References

1. Bhatt S, Gething PW, Brady OJ, Messina JP, Farlow AW, Moyes CL, Drake JM, Brownstein JS, Hoen AG, Sankoh O, et al. The global distribution and burden of dengue. Nature. 2013;496:504–7.
2. Bhatia R, Dash AP, Sunyoto T. Changing epidemiology of dengue in South-East Asia. WHO South East Asia J Public Health. 2013;2:23–7.
3. Shepard DS, Undurraga EA, Halasa YA. Economic and disease burden of dengue in Southeast Asia. PLoS Negl Trop Dis. 2013;7:e2055.
4. Shepard DS, Undurraga EA, Halasa YA, Stanaway JD. The global economic burden of dengue: a systematic analysis. Lancet Infect Dis. 2016;16:935–41.
5. Balsitis SJ, Coloma J, Castro G, Alava A, Flores D, McKerrow JH, Beatty PR, Harris E. Tropism of dengue virus in mice and humans defined by viral nonstructural protein 3-specific immunostaining. Am J Trop Med Hyg. 2009;80:416–24.
6. Hall WC, Crowell TP, Watts DM, Barros VL, Kruger H, Pinheiro F, Peters CJ. Demonstration of yellow fever and dengue antigens in formalin-fixed paraffin-embedded human liver by immunohistochemical analysis. Am J Trop Med Hyg. 1991;45:408–17.
7. Nujum ZT, Thomas A, Vijayakumar K, Nair RR, Pillai MR, Indu PS, Sundar S, Gopakumar S, Mohan D, Sudheeshkumar TK. Comparative performance of the probable case definitions of dengue by WHO (2009) and the WHO-SEAR expert group (2011). Pathog Glob Health. 2014;108:103–10.
8. Thein TL, Leo YS, Lee VJ, Sun Y, Lye DC. Validation of probability equation and decision tree in predicting subsequent dengue hemorrhagic fever in adult dengue inpatients in Singapore. Am J Trop Med Hyg. 2011;85:942–5.
9. Johnson AJ, Roehrig JT. New mouse model for dengue virus vaccine testing. J Virol. 1999;73:783–6.
10. Clapham HE, Rodriguez-Barraquer I, Azman AS, Althouse BM, Salje H, Gibbons RV, Rothman AL, Jarman RG, Nisalak A, Thaisomboonsuk B, et al. Dengue Virus (DENV) neutralizing antibody kinetics in children after symptomatic primary and Postprimary DENV infection. J Infect Dis. 2016;213:1428–35.
11. Halstead SB. Neutralization and antibody-dependent enhancement of dengue viruses. Adv Virus Res. 2003;60:421–67.
12. Gan ES, Ting DH, Chan KR. The mechanistic role of antibodies to dengue virus in protection and disease pathogenesis. Expert Rev Anti Infect Ther. 2017;15:111–9.
13. St John AL, Rathore APS. Adaptive immune responses to primary and secondary dengue virus infections. Nat Rev. 2019;19:218–30.
14. Hatch S, Endy TP, Thomas S, Mathew A, Potts J, Pazoles P, Libraty DH, Gibbons R, Rothman AL. Intracellular cytokine production by dengue virus-specific T cells correlates with subclinical secondary infection. J Infect Dis. 2011;203:1282–91.

Ioannidis *et al. Journal of Biomedical Science*   (2023) 30:24

Page 19 of 21

15. Yauch LE, Zellweger RM, Kotturi MF, Qutubuddin A, Sidney J, Peters B, Prestwood TR, Sette A, Shresta S. A protective role for dengue virus-specific CD8$^+$ T cells. J Immunol. 2009;182:4865–73.

16. Weiskopf D, Sette A. T-cell immunity to infection with dengue virus in humans. Front Immunol. 2014;5:93.

17. Mongkolsapaya J, Dejnirattisai W, Xu XN, Vasanawathana S, Tangthawornchaikul N, Chairunsri A, Sawasdivorn S, Duangchinda T, Dong T, Rowland-Jones S, et al. Original antigenic sin and apoptosis in the pathogenesis of dengue hemorrhagic fever. Nat Med. 2003;9:921–7.

18. Duangchinda T, Dejnirattisai W, Vasanawathana S, Limpitikul W, Tangthawornchaikul N, Malasit P, Mongkolsapaya J, Screaton G. Immunodominant T-cell responses to dengue virus NS3 are associated with DHF. Proc Natl Acad Sci USA. 2010;107:16922–7.

19. Culshaw A, Ladell K, Gras S, McLaren JE, Miners KL, Farenc C, van den Heuvel H, Gostick E, Dejnirattisai W, Wangteeraprasert A, et al. Germline bias dictates cross-serotype reactivity in a common dengue-virus-specific CD8(+) T cell response. Nat Immunol. 2017;18:1228–37.

20. Mangada MM, Rothman AL. Altered cytokine responses of dengue-specific CD4$^+$ T cells to heterologous serotypes. J Immunol. 2005;175(4):2676–83.

21. Suwarto S, Nainggolan L, Sinto R, Effendi B, Ibrahim E, Suryamin M, Sasmono RT. Dengue score: a proposed diagnostic predictor for pleural effusion and/or ascites in adults with dengue infection. BMC Infect Dis. 2016;16:322.

22. Office WHOSEAR. Comprehensive guidelines for prevention and control of dengue and dengue haemorrhagic fever. Revised and expanded edition. In. New Delhi:World Health Organization; 2011.

23. Finck R, Simonds EF, Jager A, Krishnaswamy S, Sachs K, Fantl W, Pe'er D, Nolan GP, Bendall SC. Normalization of mass cytometry data with bead standards. Cytometry A. 2013;83:483–94.

24. Kotecha N, Krutzik PO, Irish JM. Web-based analysis and publication of flow cytometry experiments.Curr Protoc Cytom 2010, Chap.10:Unit10 17.

25. Amir el AD, Davis KL, Tadmor MD, Simonds EF, Levine JH, Bendall SC, Shenfeld DK, Krishnaswamy S, Nolan GP. Pe'er D: viSNE enables visualization of high dimensional single-cell data and reveals phenotypic heterogeneity of leukemia. Nat Biotechnol. 2013;31:545–52.

26. Van Gassen S, Callebaut B, Van Helden MJ, Lambrecht BN, Demeester P, Dhaene T, Saeys Y. FlowSOM: using self-organizing maps for visualization and interpretation of cytometry data. Cytometry A. 2015;87:636–45.

27. Bruggner RV, Bodenmiller B, Dill DL, Tibshirani RJ, Nolan GP. Automated identification of stratifying signatures in cellular subpopulations. Proc Natl Acad Sci U S A. 2014;111:E2770-2777.

28. Liao Y, Smyth GK, Shi W. The subread aligner: fast, accurate and scalable read mapping by seed-and-vote. Nucleic Acids Res. 2013;41:e108.

29. Liao Y, Smyth GK, Shi W. The R package rsubread is easier, faster, cheaper and better for alignment and quantification of RNA sequencing reads. Nucleic Acids Res. 2019;47:e47.

30. Liao Y, Smyth GK, Shi W. featureCounts: an efficient general purpose program for assigning sequence reads to genomic features. Bioinformatics. 2014;30:923–30.

31. Robinson MD, McCarthy DJ, Smyth GK. edgeR: a Bioconductor package for differential expression analysis of digital gene expression data. Bioinformatics. 2010;26:139–40.

32. Robinson MD, Oshlack A. A scaling normalization method for differential expression analysis of RNA-seq data. Genome Biol. 2010;11:R25.

33. Law CW, Chen Y, Shi W, Smyth GK. Voom: Precision weights unlock linear model analysis tools for RNA-seq read counts. Genome Biol. 2014;15:R29.

34. Liu R, Holik AZ, Su S, Jansz N, Chen K, Leong HS, Blewitt ME, Asselin-Labat ML, Smyth GK, Ritchie ME. Why weight? Modelling sample and observational level variability improves power in RNA-seq analyses. Nucleic Acids Res. 2015;43:e97.

35. Ritchie ME, Phipson B, Wu D, Hu Y, Law CW, Shi W. Smyth GK: limma powers differential expression analyses for RNA-sequencing and microarray studies. Nucleic Acids Res. 2015;43:e47.

36. Smyth GK. Linear models and empirical bayes methods for assessing differential expression in microarray experiments. Stat Appl Genet Mol Biol. 2004;3:Article3.

37. Young MD, Wakefield MJ, Smyth GK, Oshlack A. Gene ontology analysis for RNA-seq: accounting for selection bias. Genome Biol. 2010;11:R14.

38. Weiner J, Domaszewska T. tmod: an R package for general and multivariate enrichment analysis. PeerJ Preprints. 2016;September:1–9.

39. Li S, Rouphael N, Duraisingham S, Romero-Steiner S, Presnell S, Davis C, Schmidt DS, Johnson SE, Milton A, Rajam G, et al. Molecular signatures of antibody responses derived from a systems biology study of five human vaccines. Nat Immunol. 2014;15:195–204.

40. Liberzon A, Subramanian A, Pinchback R, Thorvaldsdottir H, Tamayo P, Mesirov JP. Molecular signatures database (MSigDB) 3.0. Bioinformatics. 2011;27:1739–40.

41. Subramanian A, Tamayo P, Mootha VK, Mukherjee S, Ebert BL, Gillette MA, Paulovich A, Pomeroy SL, Golub TR, Lander ES, et al. Gene set enrichment analysis: a knowledge-based approach for interpreting genome-wide expression profiles. Proc Natl Acad Sci USA. 2005;102:15545–50.

42. Walter W, Sanchez-Cabo F, Ricote M. GOplot: an R package for visually combining expression data with functional analysis. Bioinformatics. 2015;31:2912–4.

43. Gu Z, Eils R, Schlesner M. Complex heatmaps reveal patterns and correlations in multidimensional genomic data. Bioinformatics. 2016;32:2847–9.

44. Gu Z, Gu L, Eils R, Schlesner M, Brors B. Circlize implements and enhances circular visualization in R. Bioinformatics. 2014;30:2811–2.

45. Benjamini Y. Y H: Controlling the False Discovery Rate - a Practical and Powerful Approach to Multiple Testing. 1995,J R Stat Soc:289–300.

46. Kuss-Duerkop SK, Wang J, Mena I, White K, Metreveli G, Sakthivel R, Mata MA, Munoz-Moreno R, Chen X, Krammer F, et al. Influenza virus differentially activates mTORC1 and mTORC2 signaling to maximize late stage replication. PLoS Pathog. 2017;13:e1006635.

47. Meade N, Furey C, Li H, Verma R, Chai Q, Rollins MG, DiGiuseppe S, Naghavi MH, Walsh D. Poxviruses Evade Cytosolic sensing through disruption of an mTORC1-mTORC2 Regulatory Circuit. Cell. 2018;174:1143-1157e1117.

48. Suzuki Y, Chin WX, Han Q, Ichiyama K, Lee CH, Eyo ZW, Ebina H, Takahashi H, Takahashi C, Tan BH, et al. Characterization of RyDEN (C19orf66) as an interferon-stimulated cellular inhibitor against dengue virus replication. PLoS Pathog. 2016;12:e1005357.

49. Ma CS, Avery DT, Chan A, Batten M, Bustamante J, Boisson-Dupuis S, Arkwright PD, Kreins AY, Averbuch D, Engelhard D, et al. Functional STAT3 deficiency compromises the generation of human T follicular helper cells. Blood. 2012;119:3997–4008.

50. Tsalik EL, Fiorino C, Aqeel A, Liu Y, Henao R, Ko ER, Burke TW, Reller ME, Bodinayake CK, Nagahawatte A, et al. The host response to viral infections reveals common and virus-specific signatures in the peripheral blood. Front Immunol. 2021;12:741837.

51. Liu YE, Saul S, Rao AM, Robinson ML, Agudelo Rojas OL, Sanz AM, Verghese M, Solis D, Sibai M, Huang CH, et al. An 8-gene machine learning model improves clinical prediction of severe dengue progression. Genome Med. 2022;14:33.

52. Robinson M, Sweeney TE, Barouch-Bentov R, Sahoo MK, Kalesinskas L, Vallania F, Sanz AM, Ortiz-Lasso E, Albornoz LL, Rosso F, et al. A 20-Gene set predictive of progression to severe dengue. Cell Rep. 2019;26:1104-1111e1104.

53. Banerjee A, Shukla S, Pandey AD, Goswami S, Bandyopadhyay B, Ramachandran V, Das S, Malhotra A, Agarwal A, Adhikari S, et al. RNA-Seq analysis of peripheral blood mononuclear cells reveals unique transcriptional signatures associated with disease progression in dengue patients. Transl Res. 2017;186:62-78e69.

54. Devignot S, Sapet C, Duong V, Bergon A, Rihet P, Ong S, Lorn PT, Chroeung N, Ngeav S, Tolou HJ, et al. Genome-wide expression profiling deciphers host responses altered during dengue shock syndrome and reveals the role of innate immunity in severe dengue. PLoS ONE. 2010;5:e11671.

55. Hoang LT, Lynn DJ, Henn M, Birren BW, Lennon NJ, Le PT, Duong KT, Nguyen TT, Mai LN, Farrar JJ, et al. The early whole-blood transcriptional signature of dengue virus and features associated with progression to dengue shock syndrome in vietnamese children and young adults. J Virol. 2010;84:12982–94.

56. Kwissa M, Nakaya HI, Onlamoon N, Wrammert J, Villinger F, Perng GC, Yoksan S, Pattanapanyasat K, Chokephaibulkit K, Ahmed R, et al. Dengue virus infection induces expansion of a CD14$^+$CD16$^+$ monocyte population that stimulates plasmablast differentiation. Cell Host Microbe. 2014;16:115–27.

57. Loke P, Hammond SN, Leung JM, Kim CC, Batra S, Rocha C, Balmaseda A, Harris E. Gene expression patterns of dengue virus-infected children from nicaragua reveal a distinct signature of increased metabolism. PLoS Negl Trop Dis. 2010;4:e710.

Ioannidis *et al. Journal of Biomedical Science*   (2023) 30:24

Page 20 of 21

58. Long HT, Hibberd ML, Hien TT, Dung NM, Van Ngoc T, Farrar J, Wills B, Simmons CP. Patterns of gene transcript abundance in the blood of children with severe or uncomplicated dengue highlight differences in disease evolution and host response to dengue virus infection. J Infect Dis. 2009;199:537–46.

59. Nascimento EJ, Braga-Neto U, Calzavara-Silva CE, Gomes AL, Abath FG, Brito CA, Cordeiro MT, Silva AM, Magalhaes C, Andrade R, et al. Gene expression profiling during early acute febrile stage of dengue infection can predict the disease outcome. PLoS ONE. 2009;4:e7892.

60. Popper SJ, Gordon A, Liu M, Balmaseda A, Harris E, Relman DA. Temporal dynamics of the transcriptional response to dengue virus infection in nicaraguan children. PLoS Negl Trop Dis. 2012;6:e1966.

61. Simmons CP, Popper S, Dolocek C, Chau TN, Griffiths M, Dung NT, Long TH, Hoang DM, Chau NV. Thao le TT et al: patterns of host genome-wide gene transcript abundance in the peripheral blood of patients with acute dengue hemorrhagic fever. J Infect Dis. 2007;195:1097–107.

62. Simon-Loriere E, Duong V, Tawfik A, Ung S, Ly S, Casademont I, Prot M, Courtejoie N, Bleakley K, Buchy P, et al. Increased adaptive immune responses and proper feedback regulation protect against clinical dengue. Sci Transl Med. 2017; 9(405).

63. Sun P, Garcia J, Comach G, Vahey MT, Wang Z, Forshey BM, Morrison AC, Sierra G, Bazan I, Rocha C, et al. Sequential waves of gene expression in patients with clinically defined dengue illnesses reveal subtle disease phases and predict disease severity. PLoS Negl Trop Dis. 2013;7:e2298.

64. van de Weg CA, van den Ham HJ, Bijl MA, Anfasa F, Zaaraoui-Boutahar F, Dewi BE, Nainggolan L, van Osterhaus IWF, Martina AD. Time since onset of disease and individual clinical markers associate with transcriptional changes in uncomplicated dengue. PLoS Negl Trop Dis. 2015;9:e0003522.

65. Guzman MG, Alvarez M, Halstead SB. Secondary infection as a risk factor for dengue hemorrhagic fever/dengue shock syndrome: an historical perspective and role of antibody-dependent enhancement of infection. Arch Virol. 2013;158:1445–59.

66. Weiskopf D, Angelo MA, de Azeredo EL, Sidney J, Greenbaum JA, Fernando AN, Broadwater A, Kolla RV, De Silva AD, de Silva AM, et al. Comprehensive analysis of dengue virus-specific responses supports an HLA-linked protective role for CD8^{+} T cells. Proc Natl Acad Sci USA. 2013;110:E2046-2053.

67. Fink J, Gu F, Ling L, Tolfvenstam T, Olfat F, Chin KC, Aw P, George J, Kuznetsov VA, Schreiber M, et al. Host gene expression profiling of dengue virus infection in cell lines and patients. PLoS Negl Trop Dis. 2007;1:e86.

68. Zanini F, Robinson ML, Croote D, Sahoo MK, Sanz AM, Ortiz-Lasso E, Albornoz LL, Rosso F, Montoya JG, Goo L, et al. Virus-inclusive single-cell RNA sequencing reveals the molecular signature of progression to severe dengue. Proc Natl Acad Sci USA. 2018;115:E12363-9.

69. Jaiyen Y, Masrinoul P, Kalayanarooj S, Pulmanausahakul R, Ubol S. Characteristics of dengue virus-infected peripheral blood mononuclear cell death that correlates with the severity of illness. Microbiol Immunol. 2009;53:442–50.

70. Ubol S, Masrinoul P, Chaijaruwanich J, Kalayanarooj S, Charoensirisuthikul T, Kasisith J. Differences in global gene expression in peripheral blood mononuclear cells indicate a significant role of the innate responses in progression of dengue fever but not dengue hemorrhagic fever. J Infect Dis. 2008;197:1459–67.

71. Chng MHY, Lim MQ, Rouers A, Becht E, Lee B, MacAry PA, Lye DC, Leo YS, Chen J, Fink K, et al. Large-scale HLA Tetramer Tracking of T cells during dengue infection reveals broad Acute activation and differentiation into two memory cell fates. Immunity. 2019;51:1119-1135e1115.

72. Rouers A, Chng MHY, Lee B, Rajapakse MP, Kaur K, Toh YX, Sathiakumar D, Loy T, Thein TL, Lim VWX, et al. Immune cell phenotypes associated with disease severity and long-term neutralizing antibody titers after natural dengue virus infection. Cell Rep Med. 2021;2:100278.

73. Tian Y, Babor M, Lane J, Seumois G, Liang S, Goonawardhana NDS, De Silva AD, Phillips EJ, Mallal SA, da Silva Antunes R, et al. Dengue-specific CD8^{+} T cell subsets display specialized transcriptomic and TCR profiles. J Clin Invest. 2019;129:1727–41.

74. Goncalves Pereira MH, Figueiredo MM, Queiroz CP, Magalhaes TVB, Mafra A, Diniz LMO, da Costa UL, Gollob KJ, Antonelli L, Santiago HDC. T-cells producing multiple combinations of IFNgamma, TNF and IL10 are associated with mild forms of dengue infection. Immunology. 2020;160:90–102.

75. Moore TV, Clay BS, Ferreira CM, Williams JW, Rogozinska M, Cannon JL, Shilling RA, Marzo AL, Sperling AI. Protective effector memory CD4 T cells depend on ICOS for survival. PLoS ONE. 2011;6(2):e16529.

76. Blair T, Baird J, Bambina S, Kramer G, Gostissa M, Harvey CJ, Gough MJ, Crittenden MR. ICOS is upregulated on T cells following radiation and agonism combined with radiation results in enhanced tumor control. Sci Rep. 2022;12:14954.

77. Duhen R, Fesneau O, Samson KA, Frye AK, Beymer M, Rajamanickam V, Ross D, Tran E, Bernard B, Weinberg AD et al. PD-1 and ICOS coexpression identifies tumor-reactive CD4^{+} T cells in human solid tumors. J Clin Invest 2022; 132(12).

78. Metzger TC, Long H, Potluri S, Pertel T, Bailey-Bucktrout SL, Lin JC, Fu T, Sharma P, Allison JP, Feldman RM. ICOS promotes the function of CD4^{+} effector T cells during Anti-OX40-Mediated tumor rejection. Cancer Res. 2016;76:3684–9.

79. Solinas C, Gu-Trantien C, Willard-Gallo K. The rationale behind targeting the ICOS-ICOS ligand costimulatory pathway in cancer immunotherapy. ESMO Open. 2020; 5(1).

80. Yap TA, Gainor JF, Callahan MK, Falchook GS, Pachynski RK, LoRusso P, Kummar S, Gibney GT, Burris HA, Tykodi SS, et al. First-in-human phase I/II ICONIC trial of the ICOS agonist vopratelimab alone and with Nivolumab: ICOS-High CD4 T-Cell populations and predictors of response. Clin Cancer Res. 2022;28:3695–708.

81. Moir S, Ho J, Malaspina A, Wang W, DiPoto AC, O'Shea MA, Roby G, Kottilil S, Arthos J, Proschan MA, et al. Evidence for HIV-associated B cell exhaustion in a dysfunctional memory B cell compartment in HIV-infected viremic individuals. J Exp Med. 2008;205:1797–805.

82. Weiss GE, Crompton PD, Li S, Walsh LA, Moir S, Traore B, Kayentao K, Ongoiba A, Doumbo OK, Pierce SK. Atypical memory B cells are greatly expanded in individuals living in a malaria-endemic area. J Immunol. 2009;183:2176–82.

83. Rubtsova K, Rubtsov AV, Cancro MP, Marrack P. Age-Associated B cells: a T-bet-dependent effector with roles in protective and pathogenic immunity. J Immunol. 2015;195:1933–7.

84. Portugal S, Tipton CM, Sohn H, Kone Y, Wang J, Li S, Skinner J, Virtaneva K, Sturdevant DE, Porcella SF et al. Malaria-associated atypical memory B cells exhibit markedly reduced B cell receptor signaling and effector function. Elife. 2015;4.

85. Obeng-Adjei N, Portugal S, Holla P, Li S, Sohn H, Ambegaonkar A, Skinner J, Bowyer G, Doumbo OK, Traore B, et al. Malaria-induced interferon-gamma drives the expansion of Tbethi atypical memory B cells. PLoS Pathog. 2017;13:e1006576.

86. Locci M, Havenar-Daughton C, Landais E, Wu J, Kroenke MA, Arlehamn CL, Su LF, Cubas R, Davis MM, Sette A, et al. Human circulating PD-1^{+}CXCR3CXCR5[+] memory tfh cells are highly functional and correlate with broadly neutralizing HIV antibody responses. Immunity. 2013;39:758–69.

87. Haltaufderhyde K, Srikiatkhachorn A, Green S, Macareo L, Park S, Kalayanarooj S, Rothman AL, Mathew A. Activation of peripheral T follicular helper cells during Acute Dengue Virus infection. J Infect Dis. 2018;218:1675–85.

88. Wijesinghe A, Gamage J, Goonewardena H, Gomes L, Jayathilaka D, Wijeratne DT, de Alwis R, Jeewandara C, Wijewickrama A, Ogg GS, et al. Phenotype and functionality of follicular helper T cells in patients with acute dengue infection. J Biomed Sci. 2020;27:50.

89. He J, Tsai LM, Leong YA, Hu X, Ma CS, Chevalier N, Sun X, Vandenberg K, Rockman S, Ding Y, et al. Circulating precursor CCR7^{lo}PD-1^{hi} CXCR5^{+} CD4^{+} T cells indicate tfh cell activity and promote antibody responses upon antigen reexposure. Immunity. 2013;39:770–81.

90. Velu V, Mylvaganam G, Ibegbu C, Amara RR. Tfh1 cells in germinal centers during chronic HIV/SIV infection. Front Immunol. 2018;9:1272.

91. Zhang J, Liu W, Wen B, Xie T, Tang P, Hu Y, Huang L, Jin K, Zhang P, Liu Z, et al. Circulating CXCR3^{+} tfh cells positively correlate with neutralizing antibody responses in HCV-infected patients. Sci Rep. 2019;9:10090.

92. Lertjuthaporn S, Keawvichit R, Polsrila K, Sukapirom K, Chuansumrit A, Chokephaibulkit K, Ansari AA, Khowawisetsut L, Pattanapanyasat K. Kinetic changes of peripheral blood monocyte subsets and expression of co-stimulatory molecules during acute dengue virus infection. Pathogens. 2021; 10(11).

93. Maheshwari D, Saini K, Singh P, Singla M, Nayak K, Aggarwal C, Chawla YM, Bajpai P, Kaur M, Gunisetty S, et al. Contrasting behavior between the

Ioannidis *et al. Journal of Biomedical Science*   (2023) 30:24

Page 21 of 21

three human monocyte subsets in dengue pathophysiology. iScience. 2022;25:104384.

94. Naranjo-Gomez JS, Castillo JA, Rojas M, Restrepo BN, Diaz FJ, Velilla PA, Castano D. Different phenotypes of non-classical monocytes associated with systemic inflammation, endothelial alteration and hepatic compromise in patients with dengue. Immunology. 2019;156:147–63.

95. Wong KL, Chen W, Balakrishnan T, Toh YX, Fink K, Wong SC. Susceptibility and response of human blood monocyte subsets to primary dengue virus infection. PLoS ONE. 2012;7:e36435.

96. Yen YT, Chen HC, Lin YD, Shieh CC, Wu-Hsieh BA. Enhancement by tumor necrosis factor alpha of dengue virus-induced endothelial cell production of reactive nitrogen and oxygen species is key to hemorrhage development. J Virol. 2008;82:12312–24.

97. Nadjib M, Setiawan E, Putri S, Nealon J, Beucher S, Hadinegoro SR, Permanasari VY, Sari K, Wahyono TYM, Kristin E, et al. Economic burden of dengue in Indonesia. PLoS Negl Trop Dis. 2019;13:e0007038.

Publisher's Note